Chapter IV

RESULTS AND DISCUSSION

Characterization of an acidic phospholipase A_2 purified from Indian cobra (*Naja naja*) venom

&

assessment of *in vivo* toxicity, and anticoagulant activity of this anticoagulant PLA_2 in a rodent model

Chapter IV

RESULTS AND DISCUSSION: Characterization of an acidic phospholipase A_2 purified from Indian cobra (*Naja naja*) venom, and assessment of *in vivo* toxicity, and anticoagulant activity of this anticoagulant PLA_2 in a rodent model

4.1 Brief Introduction

Indian cobra (*Naja naja*) venom is enriched in many non-enzymatic (for example three finger toxins) and enzymatic toxins such as phospholipase A_2 enzymes [1-3]. The latter enzyme is one of the major constituents of most snake venoms including *N. naja* venom, by biochemical analysis which is reported to contain up to 14 isoenzymes of PLA_2 [4]. However, by proteomic analysis of *N. naja* venom from India, only 3 PLA_2 isoenzymes were identified [5-7].

The interzonal and intrazonal variations in venom composition of the Indian cobra result in differences in pathophysiological manifestations in victims [1,8,9]. Therefore, exploration of geographical variation in venom components has tremendous implications for improving production of effective antivenom to treat cobra bite patients [1,8,9].

Phospholipase A_2 (EC: 3.1.1.4), due to its crucial role in inducing various pharmacological effects in victims and its puzzling structure-function relationships, is one of the most extensively studied snake venom enzymes [4,10-17]. A single venom may contain several isoenzymes of PLA_2, and depending on their overall charge, they may be classified as acidic, basic, or neutral PLA_2 enzymes [15,17-19]. It has been well established that different PLA_2 isoenzymes of the same venom exhibit various pharmacological effects, viz. neurotoxicity, cardiotoxicity, myotoxicity, necrosis, anticoagulant, hypotensive, hemolysis, hemorrhage and edema by different mechanisms in experimental animals and victims [18,20-22]. Among the pharmacological effects, interfering with the blood coagulation system by injecting venom components is one of the important mechanisms to impede the hemostatic system of victim or prey [11-18].

Although most of the PLA_2 enzymes purified from snake venom have been demonstrated to possess anticoagulant activity [13,15-17,21]; nevertheless, most of the

PLA_2 enzymes purified from the Indian *N. naja* venom are devoid of anticoagulant activity [1,9,23,24], and only a few have been reported to show weak anticoagulant action [25]. In the present study, therefore, an effort has been made to purify a strong anticoagulant PLA_2 from the venom of the *N. naja* and characterize its anticoagulant mechanism as well as platelet modulating activity. To the best of our knowledge, this is the first report of a thrombin inhibitor PLA_2 isolated from *N. naja* venom.

4.2 Results

4.2.1 Isolation and purification of an anticoagulant PLA_2 from *N. naja* venom

4.2.1.1 Cation-exchange chromatography of *N. naja* venom

Fractionation of crude *N. naja* venom through a cation-exchange HiPrep CM FF 16/10 column (20 ml) resolved into six distinct peaks-NnCM1 – 6 (Fig. 4.1A). NnCM1 eluted with the equilibration buffer containing either neutral or acidic proteins showed the highest anticoagulant and PLA_2 activities.

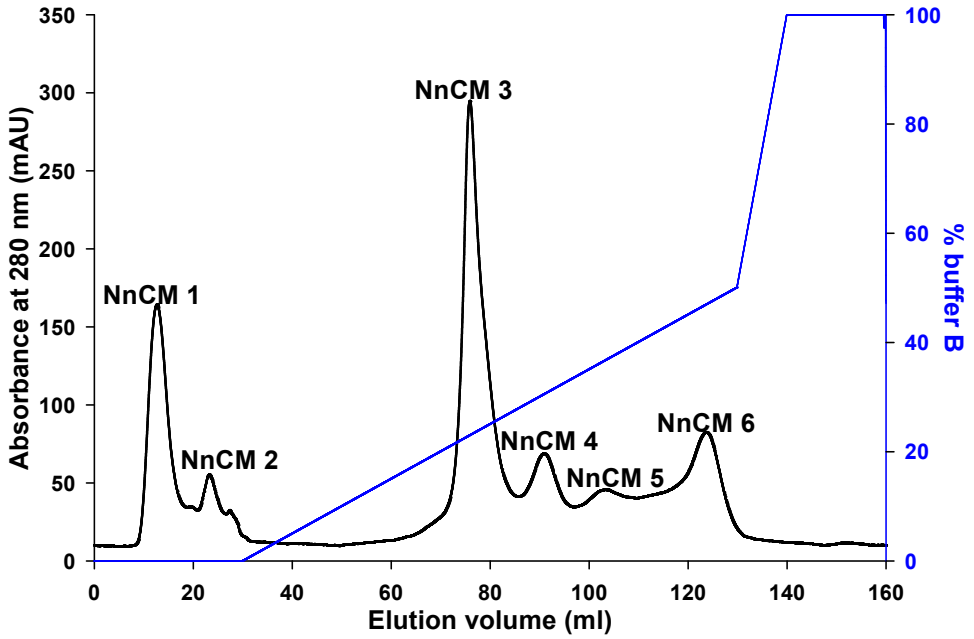

Fig 4.1A. Elution profile of cation-exchange chromatography of crude *N. naja* venom. The HiPrep CM FF 16/10 (20.0 ml) cation exchange column was pre-equilibrated with 20 mM Tris-HCl buffer, pH 7.4 (buffer A). 10 mg of crude *N. naja* venom (dry weight) was dissolved in 0.5 ml of buffer A and loaded on to the pre-

equilibrated cation-exchange column. The unbound venom proteins were eluted by a wash with buffer A for 30 min; while the bound proteins were eluted with a gradient of 1.0 M NaCl dissolved in buffer A (buffer B). The flow rate was maintained at 1.0 ml/min and fractions of 1.5 ml were collected.

4.2.1.2 Gel filtration chromatography of NnCM1

Gel filtration of the NnCM1 peak through a Sephadex G-50 (60 ml) column resolved into 8 protein peaks – NnCM1GF1 to NnCM1GF 8 (Fig 4.1B).

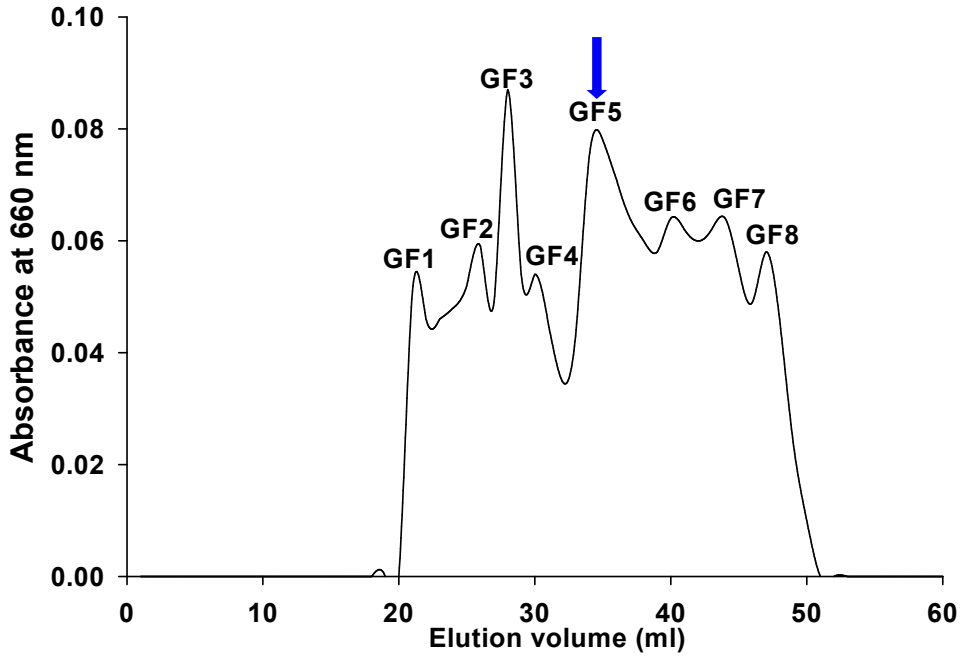

Fig 4.1B. Elution profile of gel filtration chromatography of NnCM1. 1.0 mg of pooled and lyophilized NnCM1 was re-constituted in 1.0 ml of 20 mM Tris-HCl buffer, pH 7.4 and subjected to gel filtration chromatography in a Sephadex G-50 column (60 ml) pre-equilibrated with the same buffer. The flow rate was maintained at 20 ml/h and fractions of 1.0 ml were collected.

The peak NnCM1GF5 demonstrated highest anticoagulant and PLA_2 activities. Owing to its strong PLA_2 activity, the purified protein was named $NnPLA_2$-I.

A summary of purification of this purified PLA_2 enzyme is shown in Table 4.1. The $NnPLA_2$-I represents 3.4% of total venom protein.

Table 4.1. Summary of purification of an anticoagulant PLA_2 enzyme ($NnPLA_2$-I) from *N. naja* venom.

Fraction	Total protein (mg)	% yield of protein	PLA_2 activity		Anticoagulant activity		Purification fold	
			Unit* (U)	Specific activity (U/mg)	Unit¶ (U)	Specific activity (U/mg)	PLA_2 activity	Anticoagulant activity
Crude venom	5.6	100.0	91.7	1.83×10^3	115.8	2.3×10^4	1.0	1.0
Cation-exchange fraction	3.0	53.6	91.0	3.03×10^4	134.6	4.5×10^4	16.6	1.9
Gel filtration fraction ($NnPLA_2$-I)	0.2	3.4	86.8	8.29×10^4	62.4	6.2×10^4	45.3	2.7

*Unit activity is defined as the amount of protein which produces a decrease in 0.01 absorbance in 10 min at 740 nm; ¶One unit of anticoagulant activity is defined as crude venom / venom fraction / purified PLA_2 induced 1 s increase in clotting time of the control platelet poor plasma (PPP).

Data represent a typical experiment.

4.2.2 RP-HPLC of NnCM1GF5

NnCM1GF5 ($NnPLA_2$-I), showing strong anticoagulant activity was subjected to RP-HPLC in a Dionex Acclaim C_{18} (2.1 × 150 mm, 3 µm) column which resolved into a single major peak at a retention time of 5.7 min (Fig 4.2). Elution of a single peak suggests that the preparation is pure and without contamination of other protein(s).

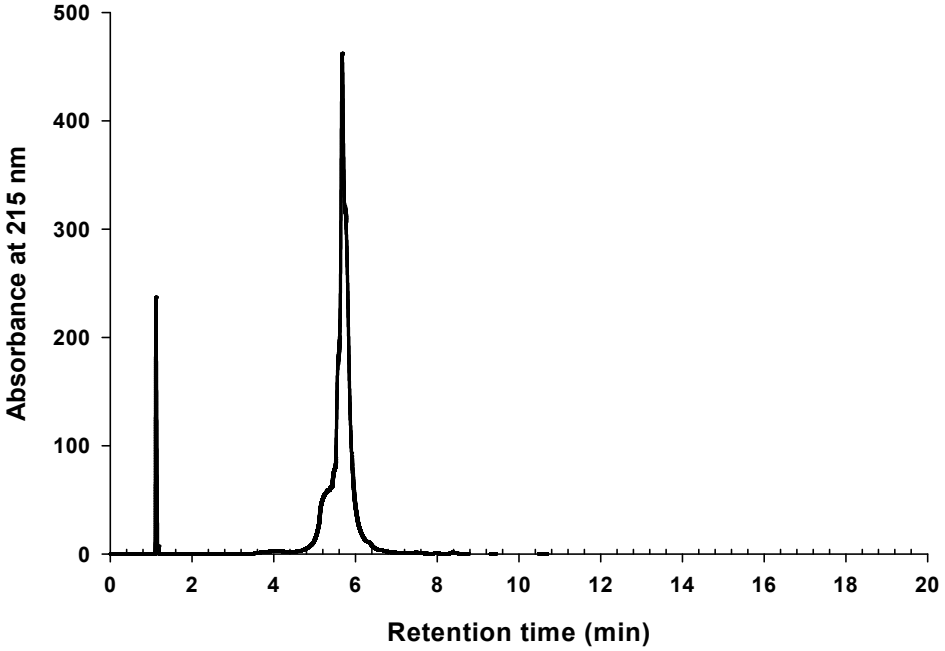

Fig 4.2. Elution profile of reversed phase-high performance liquid chromatography of NnCM1GF5 ($NnPLA_2$-I). 10.0 µg of lyophilized NnCM1GF5 was re-constituted in 10.0 µl of solvent A (Type I ultrapure water containing 0.1% 0.1% TFA) and subjected to RP-HPLC in a Dionex Acclaim C_{18} (2.1 × 150 mm, 3 µm) column coupled to an Ultimate 3000 UHPLC system pre-equilibrated with 5% solvent B (90% ACN containing 0.1% TFA). The flow rate was maintained at 0.5 ml/min.

4.2.3 Determination of molecular weight of $NnPLA_2$-I

By SDS-PAGE analysis, 30.0 µg of reduced protein ($NnPLA_2$-I) showed a sharp single band of ~15.1 kDa, whereas under non-reduced condition it displayed a diffused band of ~16 kDa (Fig. 4.3). By MALDI-ToF-MS analysis, the $NnPLA_2$-I demonstrated a doubly charged [MH^{2+}], low intensity peak at m/z 7092.5, and an [MH^{+}] peak at m/z 14186.0 (Fig. 4.4).

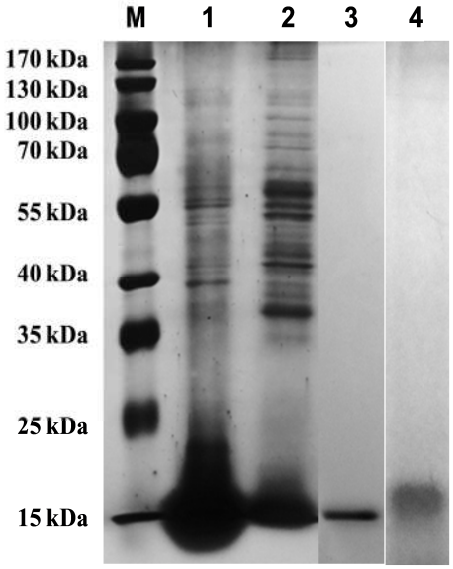

Fig 4.3. SDS-PAGE analysis of NnPLA$_2$-I. NnPLA$_2$-I, NnCM1, and *N. naja* venom was subjected to 12.5% SDS-PAGE analysis. Lane M, molecular weight marker; lane 1, reduced crude *N. naja* venom (50 µg); lane 2, reduced NnCM1 (50 µg); lane 3, reduced NnPLA$_2$-I (NnCM1GF5) (30 µg); and lane 4, non-reduced NnPLA$_2$-I (30 µg).

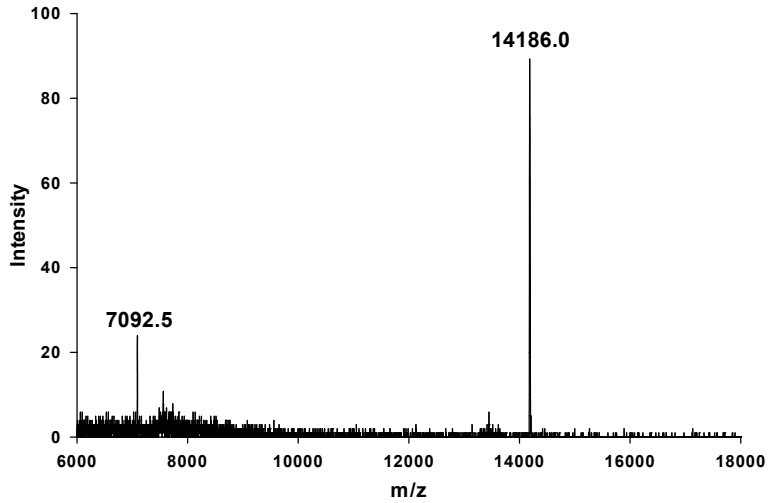

Fig 4.4. MALDI-ToF-MS analysis to determine the molecular mass of NnPLA$_2$-I. 1.0 µg of purified protein in 0.1% TFA was mixed with 1.0 µl of α-cyano-4-hydroxycinnamic acid matrix (10 mg/ml) and spotted on an Opti-TOF-384 plate (ABSciex), dried, and analyzed in a positive linear mode at an acceleration voltage of 25 kV and laser intensity of 3000. Molecular mass of the protein was determined in the range of 6000-18000 Da.

4.2.4 LC-MS/MS to identify the purified protein

The LC-MS/MS search of tryptic digested peptides of $NnPLA_2$-I showed significant similarity (rank 1, protein score 104, 100% sequence coverage) with phospholipase A_2 (MW, 13,346 Da) from *N. naja* venom (P15445) as well as with chain A, crystal structure of cobra-venom phospholipase A_2s (MW, 13,456 Da and 13,234 Da) from *N. kaouthia* (P00596, 94.96% sequence coverage) and *N. atra* (Q91133, 94.96% sequence coverage) venoms, respectively. BLAST analysis of the tryptic peptide sequences of $NnPLA_2$-I showed putative conserved domains of PLA_2-like superfamily with special reference to acidic PLA_2s from cobra venom (Table 4.2).

Table 4.2. Alignment of tryptic, semi-tryptic, and non-tryptic (*de novo*) peptide sequences of $NnPLA_2$-I with reported sequences of *Naja* sp. venom PLA_2 enzymes. The protein alignment was done using Clustal Omega programme (https://www.ebi.ac.uk /Tools/msa/clustalo/). LC-MS/MS identified peptides are marked in blue colour and substitutions are underlined.

Source organism	Accession no.	Sequence alignment
This study	$NnPLA_2$-I	NLYQFKNMIKCTVPSRSWWDFADYGCYCGRGGSGTPVDDLDRCCQVHDNCYNEAEKISGC
N. naja	P15445	NLYQFKNMIKCTVPSRSWWDFADYGCYCGRGGSGTPVDDLDRCCQVHDNCYNEAEKISGC
N. kaouthia	P00596	NLYQFKNMIQCTVPNRSWWDFADYGCYCGRGGSGTPVDDLDRCCQVHDNCYNEAEKISRC
N. atra	Q91133	NLYQFKNMIQCTVPSRSWWDFADYGCYCGRGGSGTPVDDLDRCCQVHDHCYNEAEKISGC
		*********:**********:**********
This study	$NnPLA_2$-I	WPYFKTYSYECSQGTLTCKGDNNACAASVCDCDRLAAICFAGAPYNDNNYNIDLKARCQ
N. naja	P15445	WPYFKTYSYECSQGTLTCKGDNNACAASVCDCDRLAAICFAGAPYNDNNYNIDLKARCQ
N. kaouthia	P00596	WPYFKTYSYECSQGTLTCKGDNDACAAAVCDCDRLAAICFAGAPYNNNNYNIDLKARCQ
N. atra	Q91133	WPYSKTYSYECSQGTLTCKGGNNACAAAVCDCDRLAAICFAGAPYNNNNYNIDLKARCQ
		:********:**********:**********

(*) represents identical residues in all sequences; (:) represents identical residues in at least one sequences with respect to $NnPLA_2$-I

4.2.5 Circular dichroism (CD) spectroscopy for secondary structure determination of $NnPLA_2$-I

CD analysis of $NnPLA_2$-I demonstrated the presence of 56.1% α-helix, 22.4% turns, and 21.5% random coils in its secondary structure (Fig 4.5).

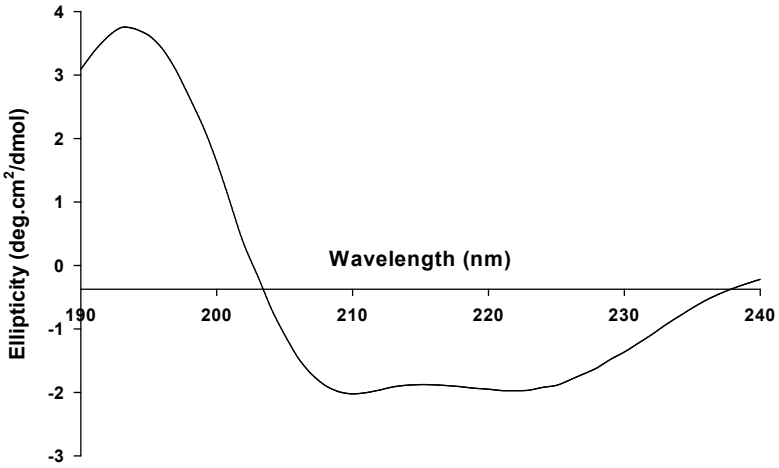

Fig. 4.5. Circular dichroism spectra of $NnPLA_2$-I demonstrating its secondary structure. $NnPLA_2$-I (0.2 mg/ml) was re-constituted in 20 mM potassium phosphate buffer, pH 7.4 and the far UV-spectra was recorded at room temperature (~25 ºC) between 190-240 nm against appropriate buffer blanks (described in section 3.2.3.2). Data represent average of four scans.

4.2.6 Biochemical characterization

4.2.6.1 Dose-dependent phospholipase A_2 activity of $NnPLA_2$-I

$NnPLA_2$-I exhibited dose-dependent increase in the phospholipids hydrolytic activity against egg-yolk suspension (Fig 4.6).

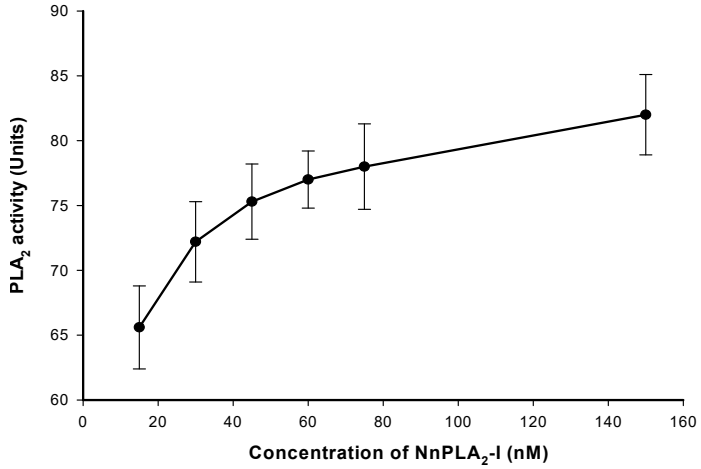

Fig 4.6. Dose-dependent phospholipid hydrolytic activity of $NnPLA_2$-I. Phospholipid hydrolysis was measured by the turbidometric method against egg-yolk suspension as described in section 3.2.5.2.1 of chapter III.

4.2.6.2 Substrate specificity of $NnPLA_2$-I

$NnPLA_2$-I preferentially hydrolyzed phosphatidylcholine (PC) over phosphatidylserine (PS) and phosphatidylethanolamine (PE) (Table 4.3). The magnitude of hydrolysis followed the order – PC > PS > PE.

Table 4.3. Substrate specificity of the acidic phospholipase A_2 ($NnPLA_2$-I) enzyme from *N. naja* venom against different substrates. Phospholipid hydrolysis activity is expressed in terms of specific activity/min. Values are mean ± SD of triplicate determinations.

Phospholipid substrate (1.0 mM)	Specific activity (U $mg^{-1}min^{-1}$)
PC	$7.4 \times 10^4 \pm 1.1 \times 10^3$
PS	$4.9 \times 10^4 \pm 1.2 \times 10^3$
PE	$2.1 \times 10^3 \pm 0.1 \times 10^2$

4.2.6.3. Kinetics of PC hydrolysis by $NnPLA_2$-I

The Michaelis-Menten plot showed that with an increase in the concentration of PC (0.5-3.0 mM), an increase in the phospholipid hydrolysis by $NnPLA_2$-I (25 nM) was observed (Fig 4.7A). A saturation of activity was observed at a PC concentration of 2.0 mM (Fig 4.7A). Using GraphPad Prism 5.0, the $1/[S]$ vs $1/V$ graph (Lineweaver-Burk plot) was plotted which provided a straight line that intersect the Y-axis at $1/Vmax$ (where $1/[S] = 0$) and the X-axis at $-1/Km$ (Fig 4.7B). From the Lineweaver-Burk plot, the *Km* and *Vmax* of $NnPLA_2$-I towards PC hydrolysis were calculated to be 0.72 mM and 29.3 μmol μg^{-1} min^{-1}.

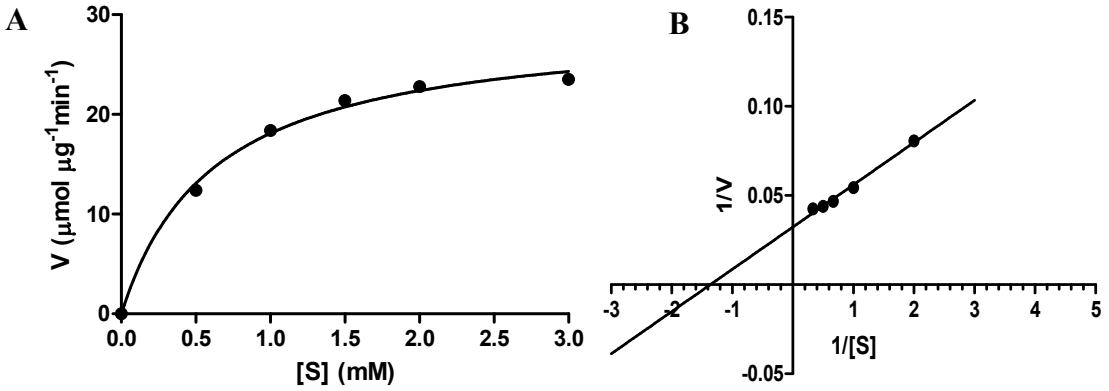

Fig 4.7. Kinetics of phosphatidylcholine (PC) hydrolysis by NnPLA$_2$-I. A. Michaelis-Menten plot to show the increase in phospholipid substrate (PC) hydrolysis by NnPLA$_2$-I with increasing concentration of the substrate. **B.** Lineweaver-Burk plot to determine the kinetic parameters (*Km* and *Vmax*) of PC hydrolysis by NnPLA$_2$-I. These plots were prepared and the parameters determined using GraphPad Prism 5.0 software with a R^2 value of 0.99 each.

4.2.6.4 Effect of temperature and pH on catalytic activity of NnPLA$_2$-I

The NnPLA$_2$-I showed optimum activity at the alkaline range with its highest activity at pH 8.0 (Fig 4.8A). Heating this PLA$_2$ for different time periods at 75 °C did not result in any significant decrease in the catalytic activity of the heated enzyme as compared to that of the control (unheated / native) enzyme (Fig 4.8B).

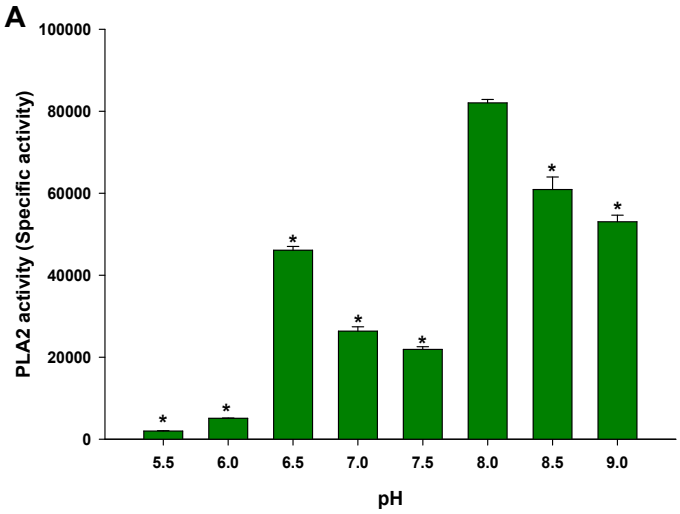

Fig 4.8A. Effect of pH on the PLA$_2$ activity of NnPLA$_2$-I. The experiments were performed as described in section 3.2.5.4 of material and methods (chapter III).

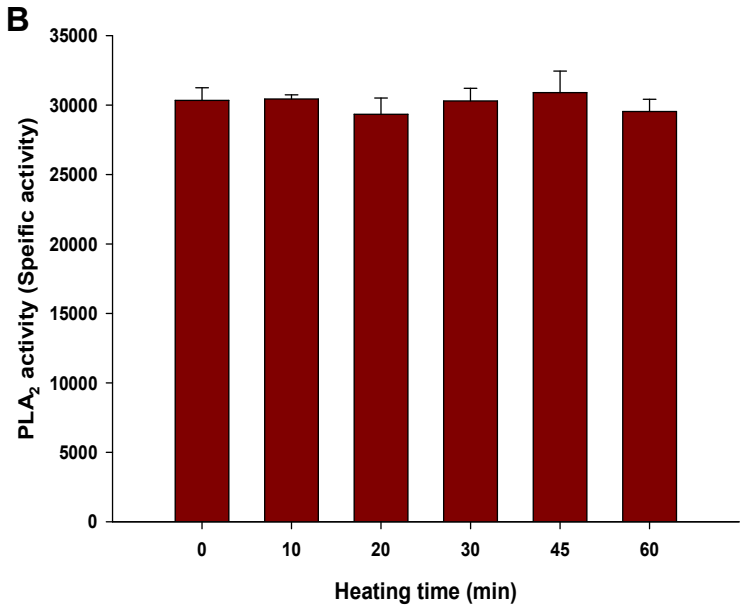

Fig 4.8B. Effect of temperature on the PLA_2 activity of $NnPLA_2$-I. The experiments were performed as described in section 3.2.5.4 of material and methods (chapter III).

4.2.7 Pharmacological characterization

4.2.7.1 Anticoagulant activity of $NnPLA_2$-I

4.2.7.1.1 Effect of $NnPLA_2$-I on re-calcification time of plasma and its comparison with commercial anticoagulants

$NnPLA_2$-I dose-dependently enhanced the re-calcification time of goat platelet poor plasma (PPP), suggesting that it is anticoagulant in nature (Fig 4.9A). A comparison of the dose-dependent anticoagulant activity of $NnPLA_2$-I with that of warfarin and heparin/AT-III is shown in Fig 4.9B. It was observed that anticoagulant activity of $NnPLA_2$-I was significantly higher ($p<0.05$) compared with that of heparin / AT-III or warfarin (Fig 4.9B).

4.2.7.1.2 Effect of $NnPLA_2$-I on PT and APTT of PPP

$NnPLA_2$-I increased the APTT of PPP in a dose-dependent manner (Fig 4.10); however, it did not affect the PT of PPP (Fig 4.10).

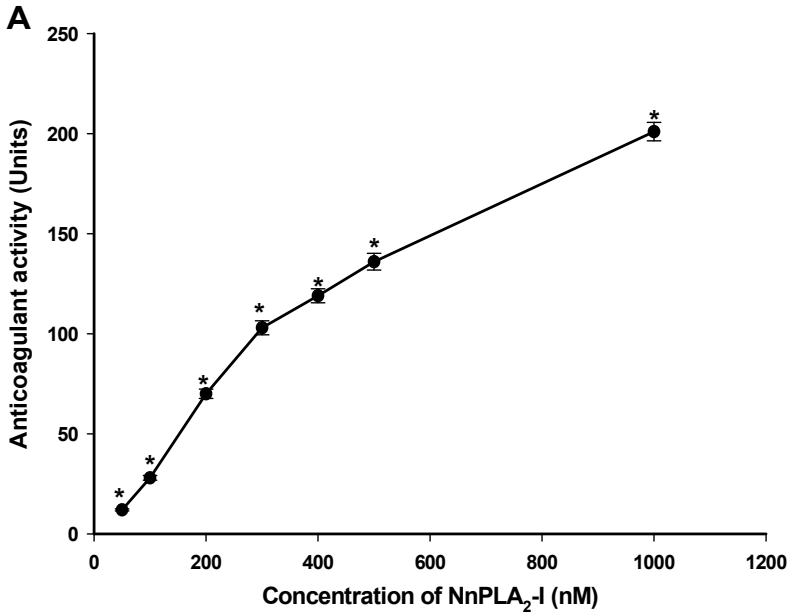

Fig 4.9A. Dose-dependent (25 – 1000 nM) effect of $NnPLA_2$-I on re-calcification time of goat PPP. The clotting time of control plasma was recorded at 97 ± 1.8 s. Values are mean ± S.D. of triplicate determinations. Significance of difference *p<0.05 as compared to control.

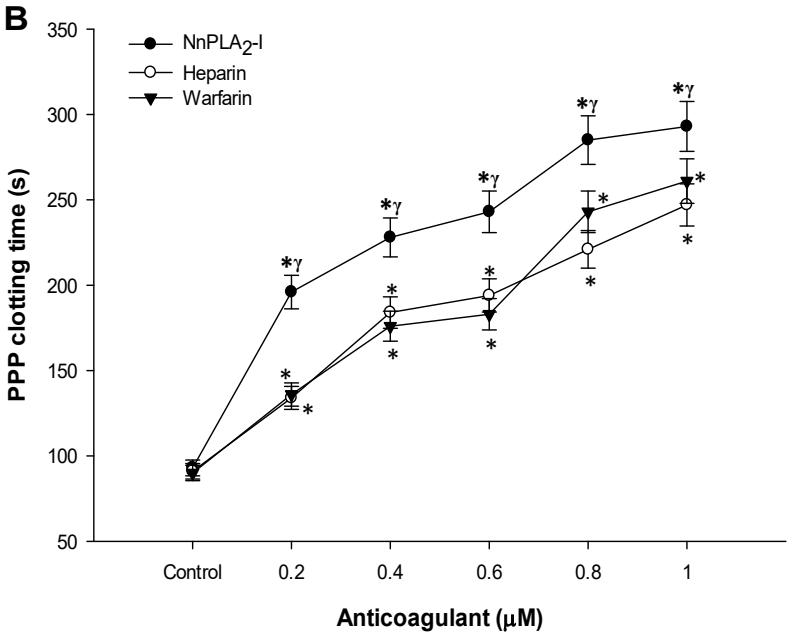

Fig 4.9B. Comparison of the dose-dependent (0.2 – 1.0 µM) anticoagulant activity of $NnPLA_2$-I (●), heparin / ATIII (○) and warfarin (▼). Values are mean ± S.D. of

triplicate determinations. Significance of difference *p<0.05 as compared to control, and $^{\gamma}$p<0.05 as compared to heparin / warfarin.

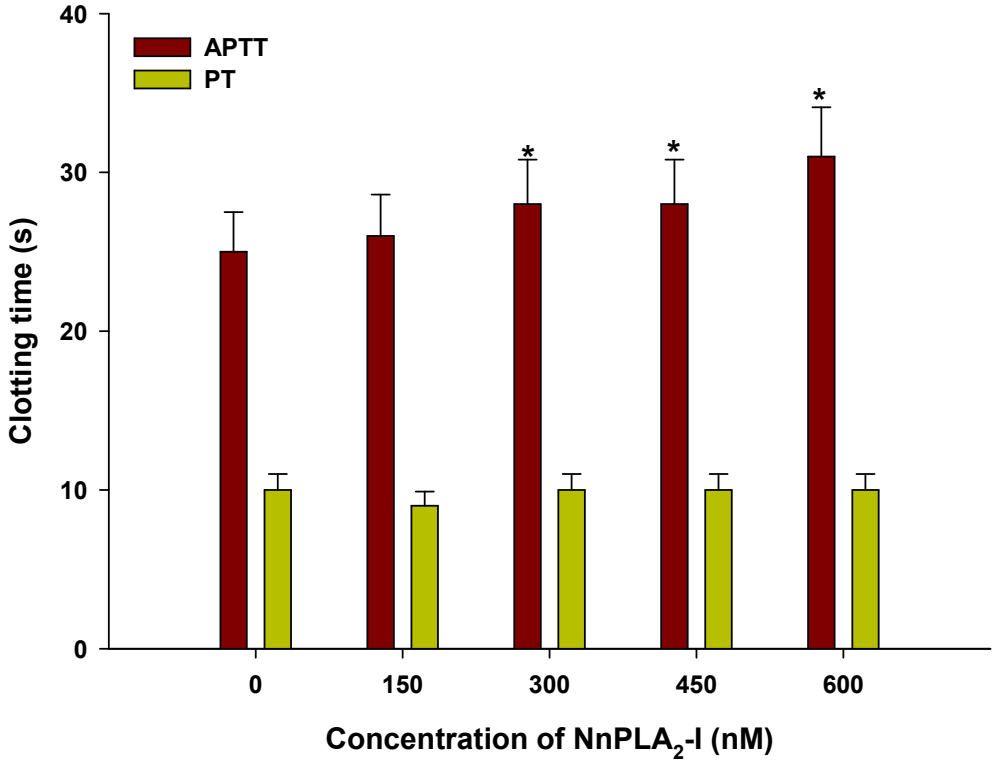

Fig 4.10. Dose-dependent (150 – 600 nM) effect of NnPLA$_2$-I on APTT and PT of goat PPP. Values are mean ± S.D. of triplicate determinations. Significance of difference as compared to control, *p<0.05.

4.2.7.2 Effect of NnPLA$_2$-I on coagulation factors

4.2.7.2.1 Effect of NnPLA$_2$-I on fibrinogen clotting time of thrombin

The NnPLA$_2$-I dose-dependently inhibited the fibrinogen clotting activity of thrombin (Fig 4.11A). Increasing the pre-incubation time of thrombin with NnPLA$_2$-I from 5 to 30 min resulted in a decrease in fibrinogen clotting activity of thrombin; the optimum inhibition being observed at 30 min of pre-incubation of thrombin with NnPLA$_2$-I (Fig. 4.11B).

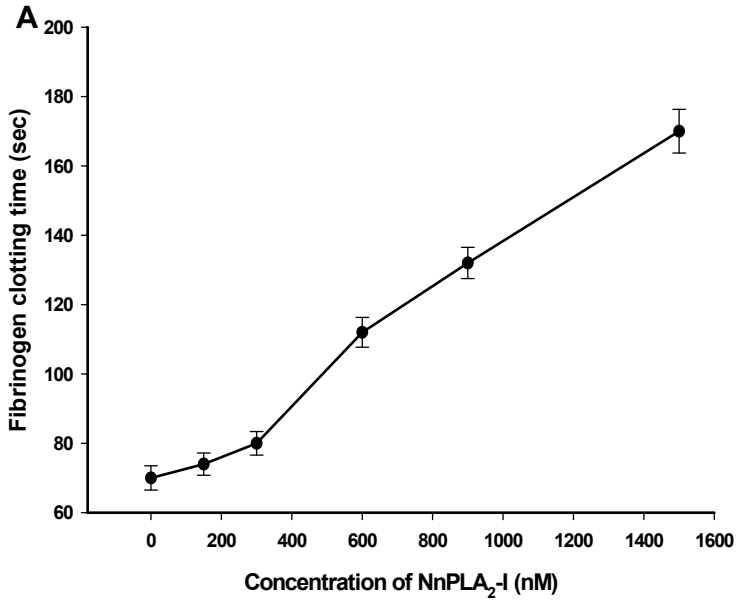

Fig 4.11A. Dose-dependent (0.15 – 1.5 µM) effect of $NnPLA_2$-I on fibrinogen clotting time of thrombin. The control (fibrinogen and thrombin) showed a clotting time of 70 ± 3.6 s. Values are mean ± SD of triplicate determinations.

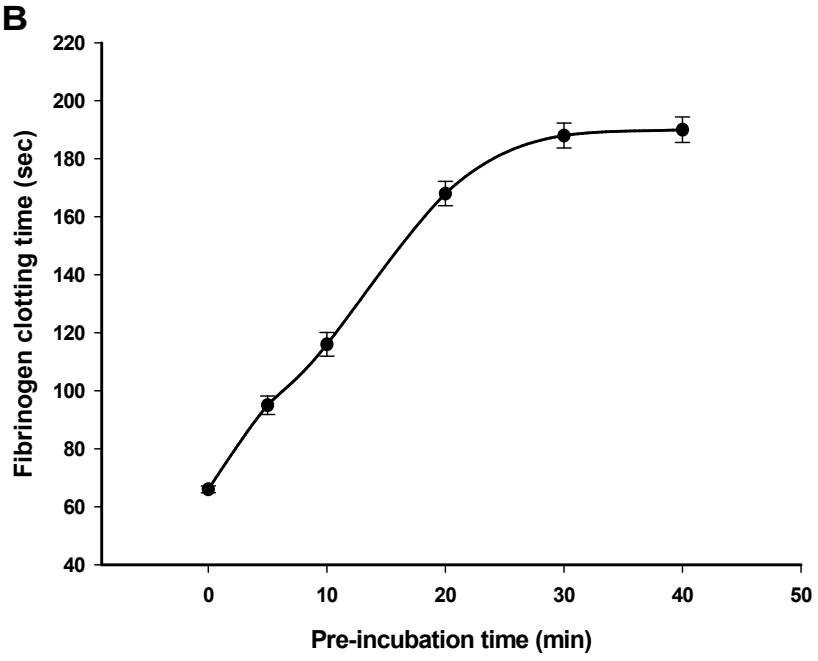

Fig 4.11B. Time-dependent (0 – 40 min) inhibition of fibrinogen clotting time of thrombin by $NnPLA_2$-I (0.5 µM). The control (fibrinogen and thrombin) showed a clotting time of 70 ± 3.6 s. Values are mean ± SD of triplicate determinations.

Treatment of $NnPLA_2$-I with *p*-BPB resulted in loss of 58 ± 2% (mean ± SD) of thrombin inhibition property of native (unmodified) $NnPLA_2$-I (100% activity).

4.2.7.2.2 Effect of $NnPLA_2$-I on amidolytic activity of thrombin

The $NnPLA_2$-I inhibited the amidolytic activity of thrombin (Fig 4.12A). It was observed that heparin or AT-III did not have any effect on the amidolytic activity of thrombin; however, together heparin and AT-III can completely eliminate the amidolytic activity of thrombin (Fig 4.12A). A comparison of thrombin inhibitory activity between $NnPLA_2$-I and heparin / AT-III showed that the latter was superior ($p<0.05$) in showing the inhibition of amidolytic activity of thrombin (Fig 4.12A). Pre-incubation of $NnPLA_2$-I with heparin resulted in a significant decrease in the thrombin inhibition property of the $NnPLA_2$-I (Fig 4.12B), suggesting that heparin has some adverse effect on anticoagulant activity of $NnPLA_2$-I. Conversely, the $NnPLA_2$-I / AT-III complex has a greater thrombin inhibition activity than the amount of thrombin inhibition shown by $NnPLA_2$-I (Fig 4.12B). Notably, the inhibition produced by heparin / AT-III / $NnPLA_2$-I complex on thrombin was superior to the same property exhibited by $NnPLA_2$-I / AT-III complex (Fig 4.12B). Nevertheless, the thrombin inhibitory effect of heparin / AT-III was found to be the best (Fig 4.12A).

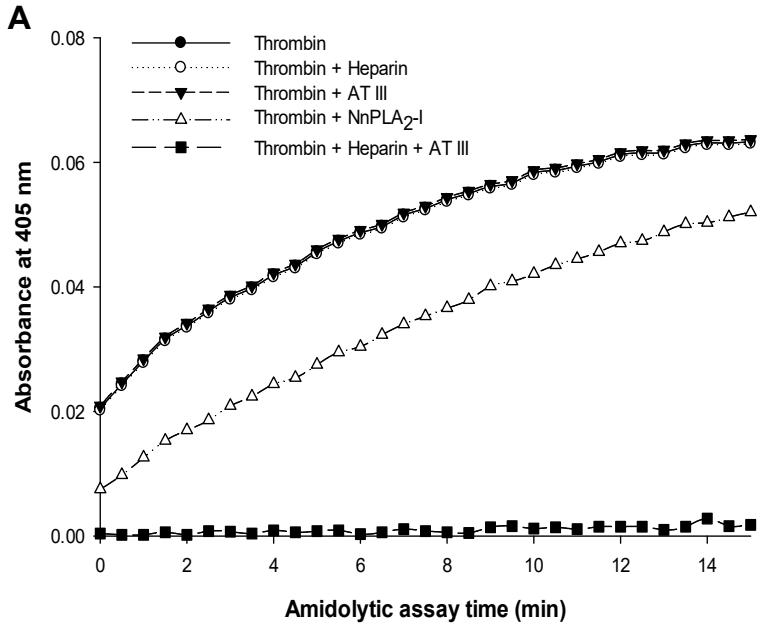

Fig 4.12A. Effect of $NnPLA_2$-I on the amidolytic activity of thrombin and its comparison to heparin / ATIII complex. A comparison of the amidolytic activity of

control thrombin (●) against its chromogenic substrate T1637 (0.2 mM in final volume); thrombin pre-incubated with 0.5 mIU of heparin (◌), thrombin pre-incubated with 2.5 μM AT III (▼), thrombin pre-incubated with 500 nM of $NnPLA_2$-I (Δ), thrombin pre-incubated with heparin / AT III (0.5 mIU/2.5 μM) complex (▲).

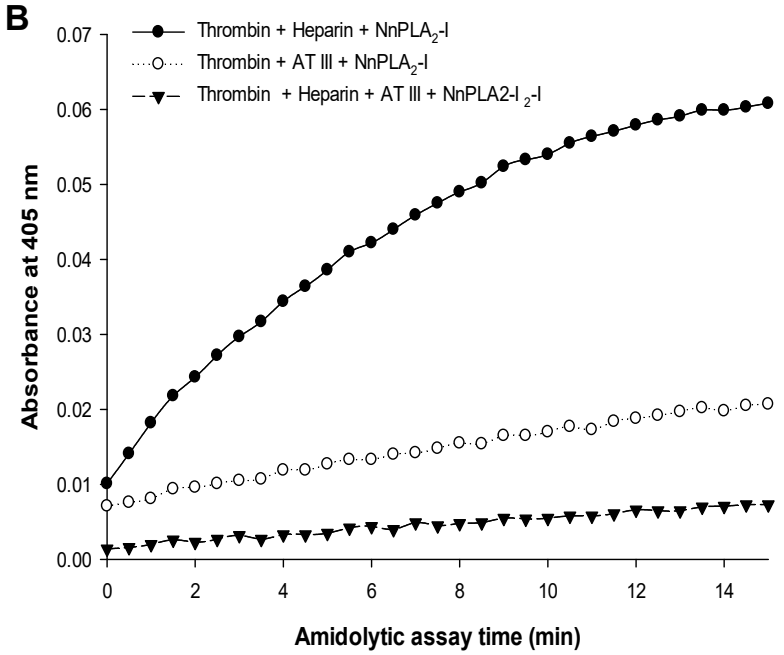

Fig 4.12B. Effect of $NnPLA_2$-I on the amidolytic activity of thrombin and its comparison to heparin / ATIII complex (contd.). A comparison of the inhibition of amidolytic activity of thrombin against its substrate T1637 when 5 nm thrombin was pre-incubated with: heparin / $NnPLA_2$-I (0.5 mIU/500 nM) (●), AT III / $NnPLA_2$-I (2.5 μM/500 nM) (◌) and heparin / AT III / $NnPLA_2$-I (0.5 mIU/2.5 μM/500 nM) (▼) complex.

4.2.7.2.3 Kinetics of thrombin inhibition by $NnPLA_2$-I

The Michaelis-Menten plot to determine the amidolytic activity of thrombin in the absence or presence of $NnPLA_2$-I (inhibitor) is shown in Fig. 4.13. The kinetic (*Km*, *Vmax* and *Kcat*) values of chromogenic substrate hydrolysis by thrombin in the absence or presence of the inhibitor ($NnPLA_2$-I) are shown in Table 4.4. It was observed that $NnPLA_2$-I produced a mixed inhibition of amidolytic activity of thrombin. The *Ki* value and α value for thrombin inhibition by $NnPLA_2$-I were determined as 9.3 ± 0.01 (mean ± SD) nM and 7.4 ± 0.7 (mean ± SD), respectively by GraphPad Prism 5.0 software.

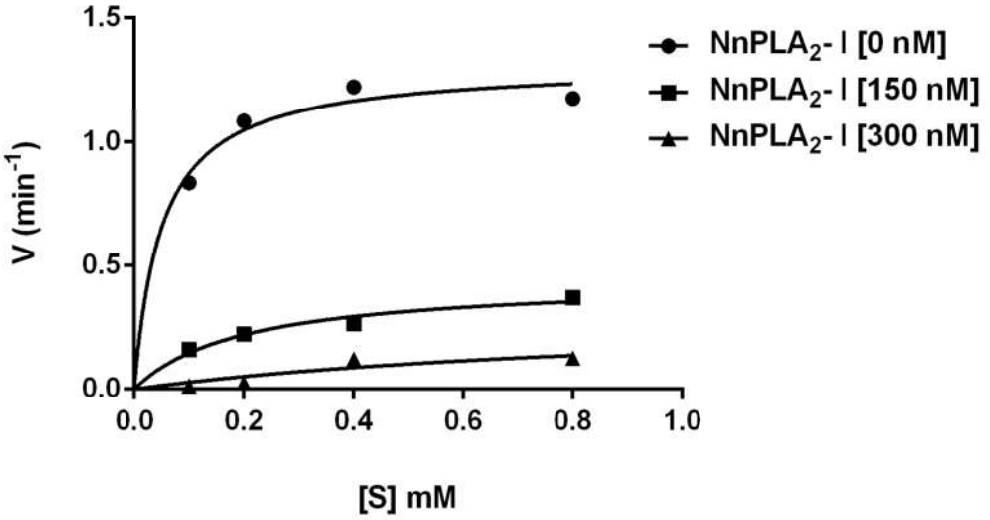

Fig 4.13. Michaelis-Menten plot for studying the kinetics of thrombin inhibition (by amidolytic activity assay) in two different inhibitor concentrations (150 nm and 300 nm) of $NnPLA_2$-I. The thrombin inhibition by $NnPLA_2$-I was assayed against different concentrations (0.1 – 0.8 mM) of the chromogenic substrate (T1637). The graph was developed using GraphPad Prism 5.0 software and the kinetic parameters were determined.

Table 4.4. Kinetics of thrombin inhibition by $NnPLA_2$-I. The kinetic parameters (*Km and Vmax*) were determined from Michaelis-Menten plot as described in the text. The values are mean ± SD of triplicate determinations.

Kinetic parameters	**Concentration of $NnPLA_2$-I (nM)**		
	0	**150**	**300**
Vmax (nmol *p*-NA min^{-1})	1.31 ± 0.08	0.44 ± 0.05	0.31 ± 0.38
Km (nM)	0.05 ± 0.02	0.20 ± 0.07	1.03 ± 1.90
Kcat (min^{-1})	7.9 ± 0.60	2.7 ± 0.20	1.9 ± 0.10

4.2.7.2.4 Effect on amidolytic and prothrombin activation property of factor Xa

Pre-incubation of FXa with $NnPLA_2$-I for 5-15 min prior to the addition to its chromogenic substrate resulted in a significant (~8 fold) increase in amidolytic activity

of FXa (Fig 4.14A). However, SDS-PAGE analysis shows that $NnPLA_2$-I did not affect the prothrombin activation property of FXa (Fig 4.14B).

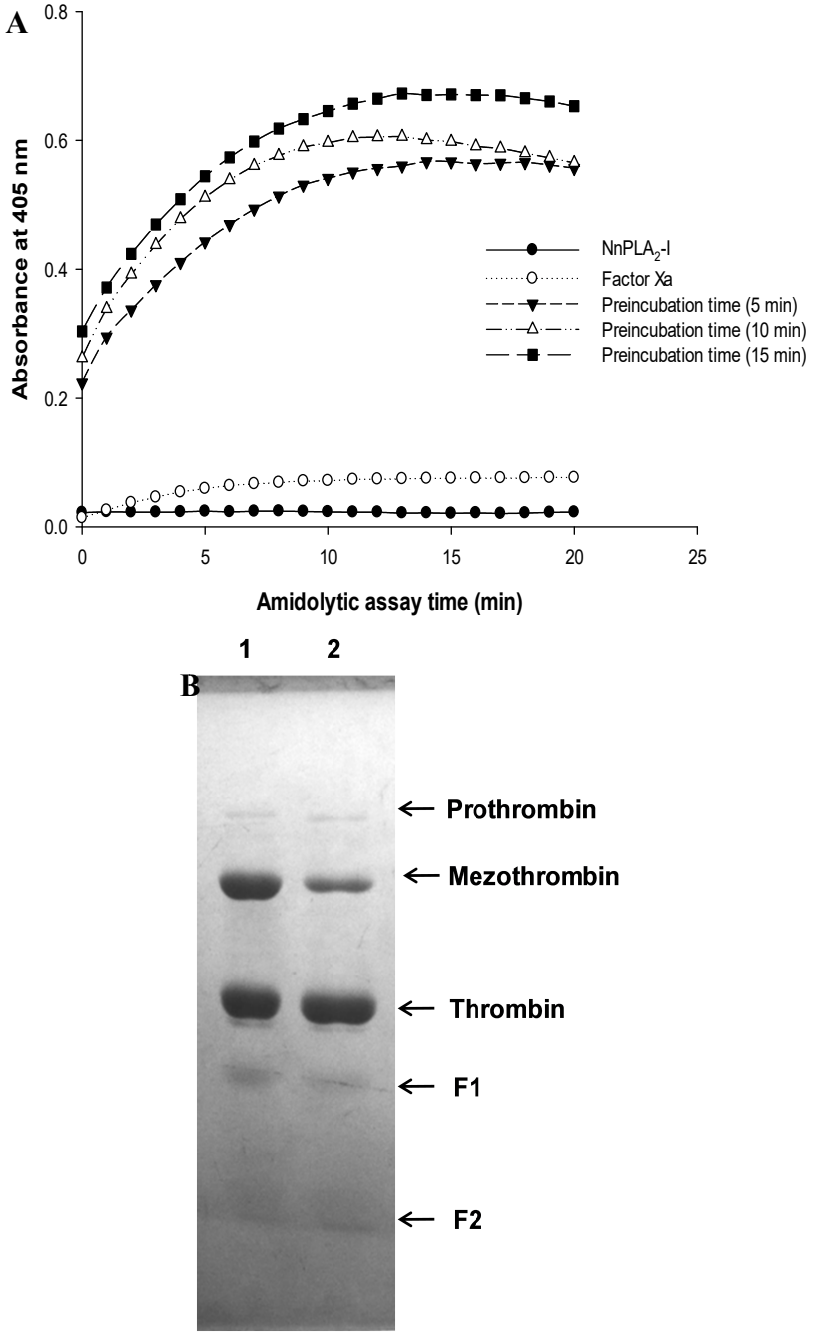

Fig 4.14. Effect of $NnPLA_2$-I on amidolytic and prothrombin activation properties of factor Xa. A. Time-dependent activation of the amidolytic activity of factor Xa (0.1 µg) by $NnPLA_2$-I (500 nM) against its chromogenic substrate F3301 (0.2 mM); **B.** The effect of $NnPLA_2$-I on the prothrombin activation by FXa as analyzed by 12.5% SDS-PAGE: lane 1, prothrombin (15 µg) incubated with factor Xa (0.1 µg), lane 2,

prothrombin (15 µg) treated with factor Xa (0.1 µg) pre-incubated with $NnPLA_2$-I (3.0 µM).

4.2.7.3 Effect on other serine proteases

The $NnPLA_2$-I was also unable to inhibit some other tested serine proteases, viz. trypsin, chymotrypsin and plasmin (Fig 4.15).

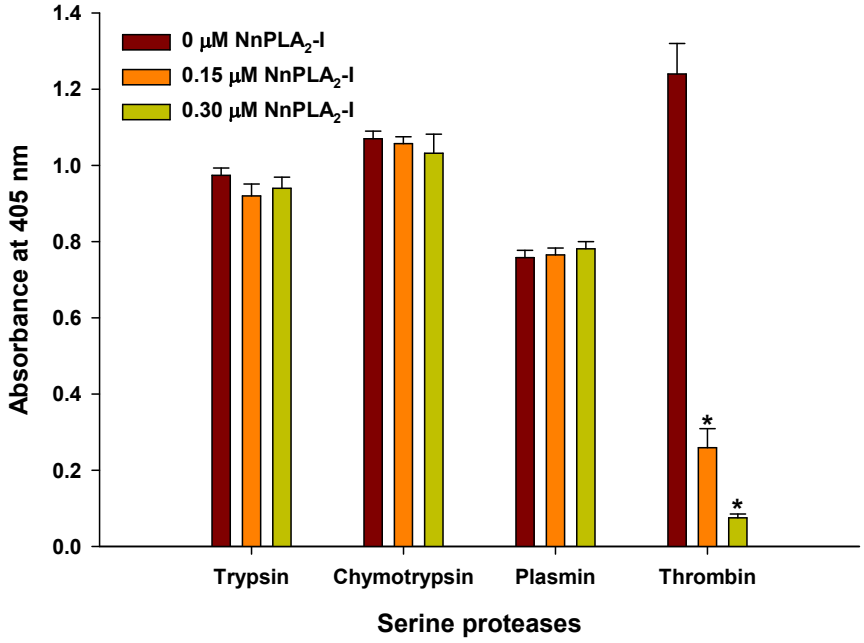

Fig 4.15. Dose-dependent (0.15 – 0.30 µM) effect of $NnPLA_2$-I on different serine proteases. Thrombin was considered as a positive control. Values are mean ± SD of triplicate determinations. Significance of difference with respect to control (without $NnPLA_2$-I), *$p<0.01$.

4.2.7.4 Platelet modulating activity of $NnPLA_2$-I

4.2.7.4.1 Effect of $NnPLA_2$-I on platelet rich plasma (PRP) and washed platelets

$NnPLA_2$-I showed dose-dependent antiplatelet effect when tested against PRP (Fig 4.16A) with an EC_{50} of 9.4 ± 0.3 nM; however, it demonstrated insignificant effect against washed platelets (Fig 4.16B). Addition of PPP or purified phospholipids PC or PS to washed platelets resulted in significant increase in deaggregation property of $NnPLA_2$-I (Fig 4.16B).

4.2.7.4.2 Effect of $NnPLA_2$-I on collagen- and thrombin-induced platelet aggregation

$NnPLA_2$-I showed inhibition of collagen-induced aggregation of PRP in a dose-dependent manner with an IC_{50} value of 4.9 nM (Fig 4.16C). Further, $NnPLA_2$-I dose-dependently inhibited the thrombin-induced aggregation of human platelets (Fig 4.16D).

4.2.7.4.3 Neutralization and inhibition of antiplatelet and platelet binding property of $NnPLA_2$-I

Incubation of PRP with *p*-BPB modified $NnPLA_2$-I resulted in a significant reduction (~95%) of platelet deaggregation property compared to that shown by the native (unmodified) enzyme (Fig 4.16E). In a sharp contrast, heparin did not interfere with the antiplatelet activity of $NnPLA_2$-I (Fig 4.16E).

It was observed that the extent of binding of both the native (unmodified) and heparin modified $NnPLA_2$-I to the washed platelets was equal; however, *p*-BPB modification resulted in ~21% inhibition of platelet binding property of $NnPLA_2$-I (Fig 4.16F).

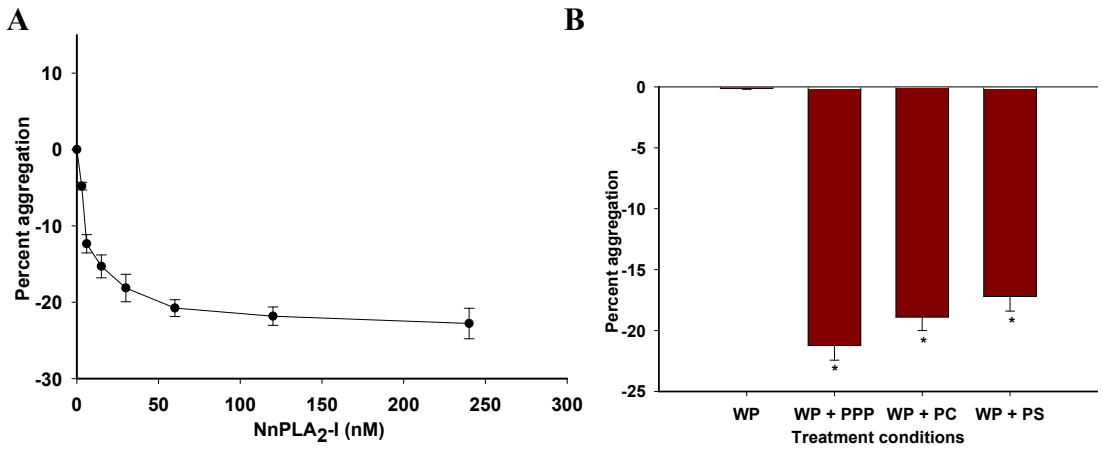

Fig 4.16. Platelet modulating activity of $NnPLA_2$-I. A. Antiplatelet activity of $NnPLA_2$-I (3 – 240 nM) on platelet rich plasma (PRP) isolated from goat blood. **B.** Effect of $NnPLA_2$-I (60 nM) on washed platelets (WP) in absence and presence of 10 µl of PPP (60 mg/ml) / PC (1.0 mM) / PS (1.0 mM). Values are mean ± SD of triplicate determinations. Significance of difference with respect to control, *$p<0.01$. The platelets were isolated by centrifuging goat PRP at 650 g for 15 min and washed after

re-suspending in Tyrode buffer by centrifuging under same conditions. Finally the platelets were suspended in Tyrode buffer and the absorbance of the suspension was adjusted to 0.15 OD at 540 nm.

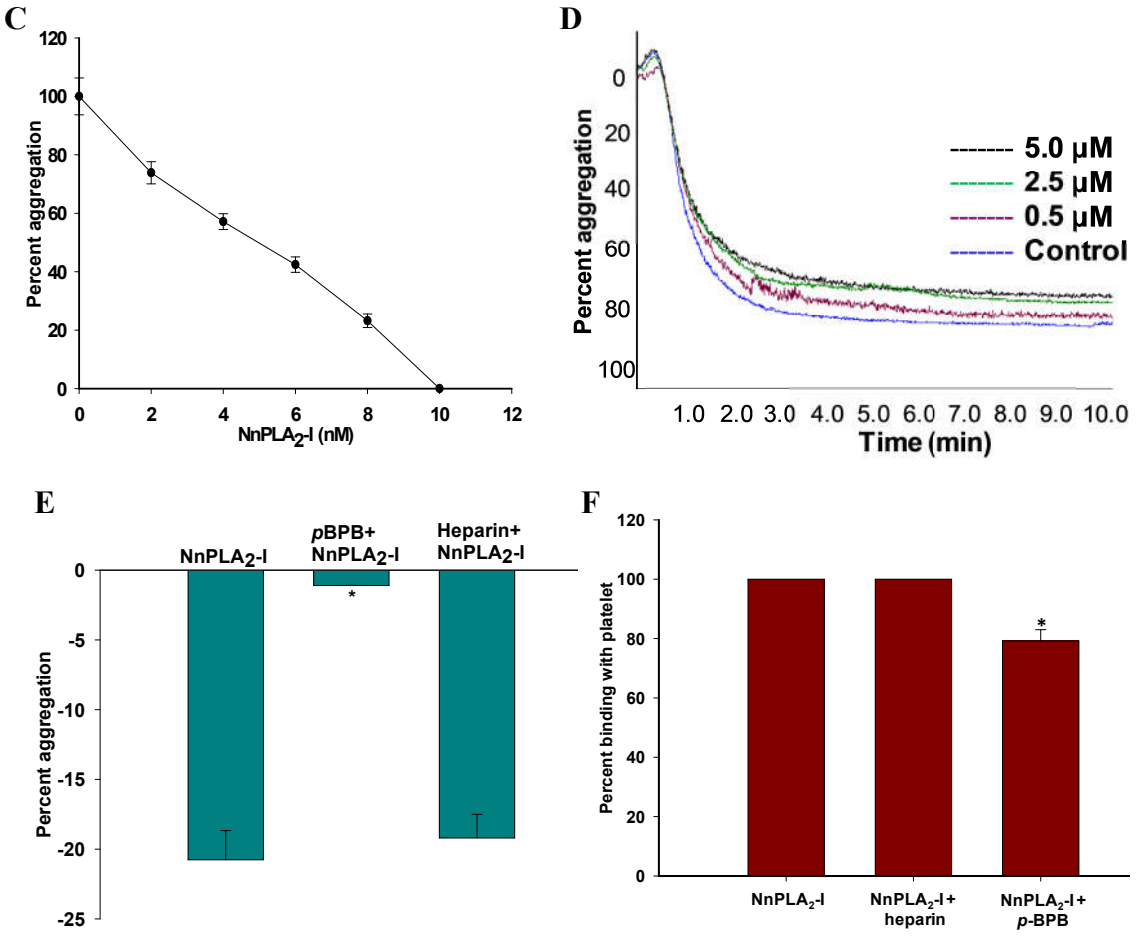

Fig 4.16. Platelet modulating activity of NnPLA$_2$-I (contd.). C. Dose-dependent effect of NnPLA$_2$-I (2 – 10 nM) on collagen (6.2 nM)-induced platelet aggregation of goat PRP. **D.** Dose-dependent effect of NnPLA$_2$-I (0.5 -5.0 µM) on human thrombin (0.20 mg/ml or 10 NIH U/ml)-induced platelet aggregation of human PRP. A range of concentrations of NnPLA$_2$-I (0.5 to 5.0 µM) was pre-incubated with human thrombin (0.20 mg/ml) for 10 min at 37 ºC prior to the addition of washed platelets. **E.** Platelet modulating activity of native and heparin (20 mIU) or *p*-BPB (2.0 mM)-treated NnPLA$_2$-I (60 nM). NnPLA$_2$-I was pre-incubated with heparin / *p*-BPB for 30 min at 37 ºC prior to addition of PRP in the reaction mixture. **F.** A comparison of platelet binding property between native NnPLA$_2$-I (250 nM) and heparin (20 mIU) or *p*-BPB (2 mM)-

treated $NnPLA_2$-I. Values are mean ± SD of triplicate determinations. Significance of difference with respect to control, *$p<0.01$.

4.2.7.5 Hemolytic activity, cell cytotoxicity, and antibacterial activity

The $NnPLA_2$-I, at a dose of 0.70 µM (10.0 µg/ml) did not exhibit hemolysis of mammalian erythrocytes or antibacterial activity against Gram positive *B. subtitlis* or Gram negative *E. coli* cells (Table 4.5). The cell viability study showed that $NnPLA_2$-I at a dose of 10.0 µg/ml (0.70 µM) failed to exhibit cytotoxicity against the tested cell lines (Table 4.5).

Table 4.5. Hemolytic, antibacterial, and *in vitro* cytotoxicity of $NnPLA_2$-I. The values are mean ± SD of triplicate determinations. ND: not detected.

Parameters analysed	**$NnPLA_2$-I (0.70 µM)** **% activity**
Hemolytic activity (goat erythrocytes), after 90 min incubation at 37 °C	
Direct	0.4 ± 0.02
Indirect	0.9 ± 0.05
Antibacterial activity	
% inhibition of growth of	
Bacillus subtilis	ND
Escherichia coli	ND
***In vitro* cytotoxicty against mammalian cell**s (post 48 h incubation at 37 °C, 5% CO_2)	
U87MG	4.6 ± 0.12
HeLa	6.5 ± 0.08
MCF-7	5.3 ± 0.04
PC-12	ND
HEK-293	1.2 ± 0.03
MEF	2.1 ± 0.07
L6	4.2 ± 0.01
Mammalian (goat) platelets	11.8 ± 0.60

The flow cytometry analysis of MCF-7 cells treated with $NnPLA_2$-I did not show significant difference ($p>0.05$) in G_1, S, and G_2 phases as compared to control cells suggesting it did not retard cell cycle of mammalian cells (Fig 4.17).

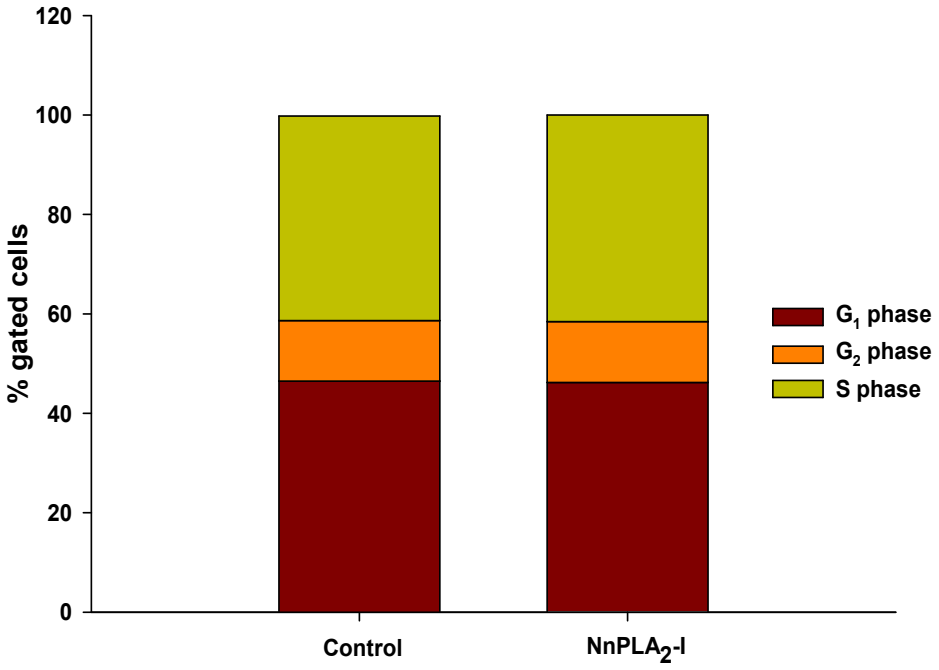

Fig 4.17. Cell cycle analysis using propidium iodide (PI) staining and flow cytometry. MCF-7 cells (1.5×10^5 cells/ml) were treated for 24 h at 37 ºC with $NnPLA_2$-I (10.0 µg/ml or 0.70 µM). Cells were harvested by trypsinization and stained with PI for 2 h and analyzed by flow cytometry.

4.2.8 Inhibition and neutralization of catalytic and anticoagulant activities of $NnPLA_2$-I

4.2.8.1 Effect of chemical inhibitors and heparin on the activities of $NnPLA_2$-I

The treatment of $NnPLA_2$-I with various chemical group modifying reagents resulted in a significant inhibition of its catalytic and anticoagulant activities, although to a different extent (Table 4.6). Interestingly, heparin differentially modulated the catalytic and anticoagulant activities of $NnPLA_2$-I. Heparin failed to inhibit the catalytic activity of $NnPLA_2$-I; however, the anticoagulant activity of $NnPLA_2$-I was inhibited by heparin to 80% of its original activity (Table 4.6).

Table 4.6. Effect of chemical inhibitors, chelating agent, and heparin on catalytic and anticoagulant activities of $NnPLA_2$-I. Values are mean ± SD of triplicate determinations. Significance of difference (Student's *t*-test) with respect to catalytic activity *p<0.01.

Inhibitors (Final Concentration)	% inhibition of activity	
	PLA_2 activity	Anticoagulant activity
p-BPB (2 mM)	96.5 ± 0.1	79.8 ± 2.1*
IAA (2 mM)	41.0 ± 0.9	55.3 ± 1.4*
EDTA (10 mM)	79.4 ± 6.2	98.1 ± 0.3*
DTT (5 mM)	97.3 ± 0.5	85.7 ± 1.2*
Heparin (20 mIU)	0	80.8 ± 4.1

4.2.8.2 Effect of heparin on thrombin inhibition by $NnPLA_2$-I

Table 4.7 shows that heparin does not have any effect on fibrinogen clotting activity of thrombin. In contrast, pre-incubation of $NnPLA_2$-I with heparin prior to the addition of thrombin significantly decreased the thrombin inhibitory activity of $NnPLA_2$-I (Table 4.7). However, neither pre-incubation of thrombin with heparin prior to the addition of $NnPLA_2$-I nor pre-incubation of thrombin with $NnPLA_2$-I prior to the addition of heparin resulted in any significant change (p>0.05) in the thrombin inhibition potency of $NnPLA_2$-I (Table 4.7).

Table 4.7. Fibrinogen clotting assay in the presence and absence of heparin. ND, not detected. The values are mean ± SD of triplicate determinations. Significance of difference *p<0.05 with respect to control and ¶p<0.05 as compared to thrombin inhibition by $NnPLA_2$-I.

Conditions	Average clotting time (s)
Control (Thrombin)	60.0 ± 5.1
(Thrombin / Heparin)	61.0 ± 6.0

(Thrombin / $NnPLA_2$-I)	275.0 ± 12.3*
($NnPLA_2$-I / Heparin) + Thrombin	119.0 ± 11.9*¶
(Thrombin / Heparin) + $NnPLA_2$-I	268.0 ± 13.8*
(Thrombin / $NnPLA_2$-I) + Heparin	266.0 ± 14.0*
Heparin	ND
$NnPLA_2$-I	ND

The response (% residual thrombin inhibition by $NnPLA_2$-I) was plotted as a function of concentration of inhibitor (heparin) using GraphPad Prism 5.0 software (Fig 4.18). A regression line was obtained with the following equation –

$y = 3.0484x + 3.358$

From the above graph, the IC_{50} value of heparin to inhibit the $NnPLA_2$-I was determined to be 15.23 mIU.

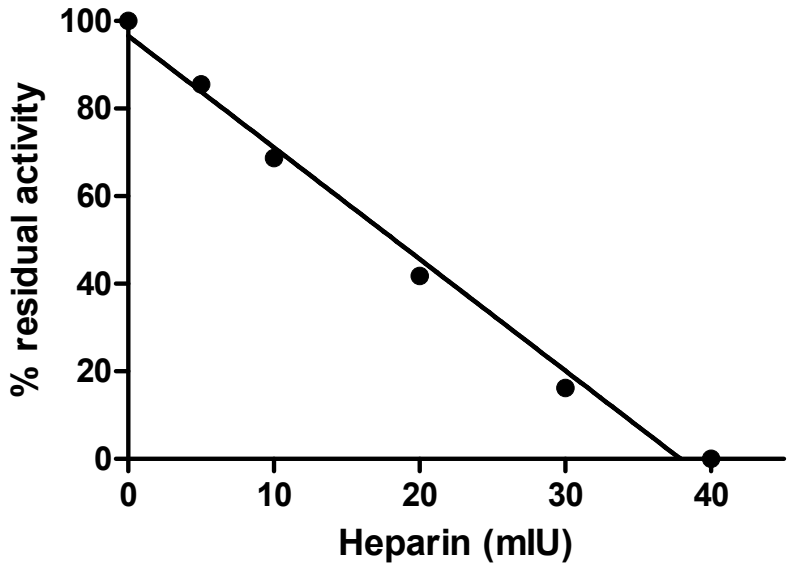

Fig 4.18. Dose (concentration of heparin) vs response (% residual activity) curve of inhibition of $NnPLA_2$-I induced thrombin inhibition by heparin. The regression line shows was plotted using GraphPad Prism 5.0 software with a R^2 value of 0.99.

4.2.8.3 Neutralization of catalytic and anticoagulant activities of $NnPLA_2$-I by commercial antivenoms

A comparison of the neutralization potency of polyvalent (PAV) versus monovalent antivenoms (MAV) shows that MAV was more efficient than PAV in neutralizing the catalytic as well as anticoagulant activities of $NnPLA_2$-I (Table 4.8). Both the antivenoms at a ratio of 1:100 differentially inhibited the catalytic as well as anticoagulant activities of $NnPLA_2$-I. With a further increase in the dose of antivenom (PAV and MAV), almost an equal inhibition of catalytic and anticoagulant activities of $NnPLA_2$-I was observed (Table 4.8).

Table 4.8. A comparison of neutralization potency of catalytic and anticoagulant activities of $NnPLA_2$-I by commercial polyvalent and monovalent antivenoms. Values are mean ± SD of triplicate determinations. Significance of difference (Student's *t*-test) with respect to inhibition by monovalent antivenom $^{¶}p<0.01$. Significance of difference (Student's *t*-test) with respect to inhibition of PLA_2 activity $^{†}p<0.01$; $^{*}p<0.05$

	% inhibition of activity (Monovalent antivenom)		% inhibition of activity (Polyvalent antivenom)	
Ratio (PLA_2:AV)	**PLA_2 activity**	**Anticoagulant activity**	**PLA_2 activity**	**Anticoagulant activity**
1:50	7.9 ± 1.3	50.3 ± 3.1†	5.9 ± 1.2	41.7 ± 3.7†
1:100	77.0 ± 3.2	88.8 ± 0.0*	23.4 ± 3.1¶	53.1 ± 3.3†¶
1:200	95.1 ± 3.1	91.7 ± 7.9	72.9 ± 4.6¶	76.9 ± 4.6¶
1:500	100	100	98.4 ± 0.2	97.4 ± 2.2

However, incubation of $NnPLA_2$-I with MAV at 1: 50 (protein: protein) did not inhibit its platelet deaggregation property; conversely, PAV under the identical experimental conditions enhanced the deaggregation property of $NnPLA_2$-I (Fig 4.19).

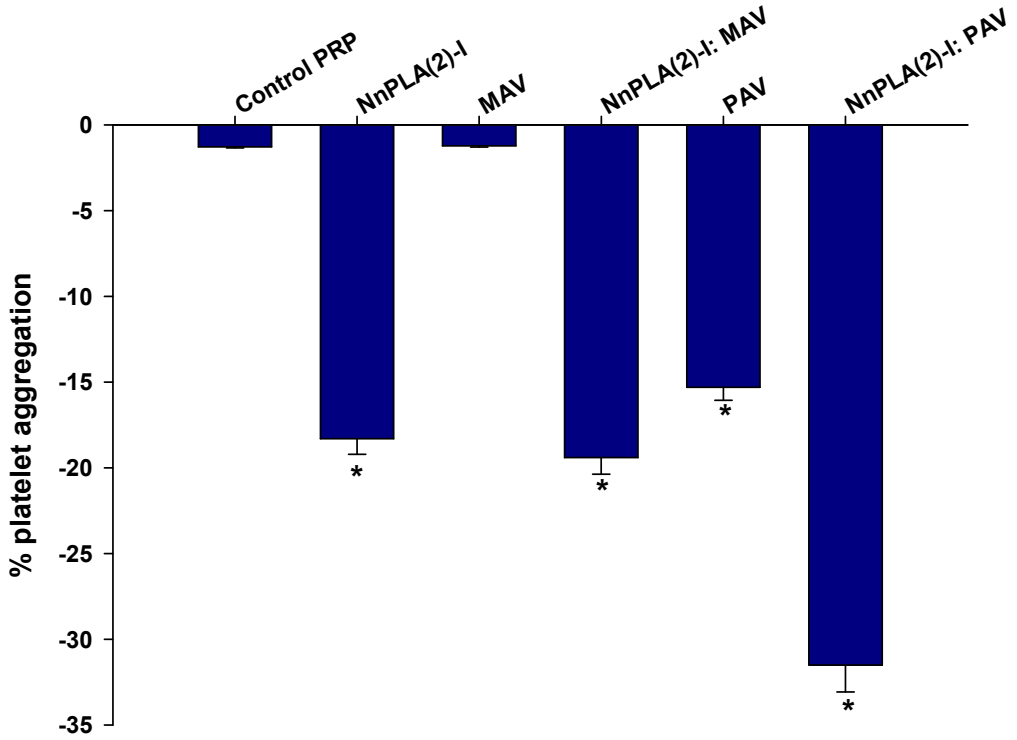

Fig 4.19. Effect of commercial antivenoms on antiplatelet property of $NnPLA_2$-I. $NnPLA_2$-I (10 nM) was incubated with MAV or PAV at a ratio of 1:25 (w/w). Values are mean ± SD of triplicate determinations. Significance of difference *$p<0.01$ with respect to control.

4.2.9 Interaction with phospholipids and coagulation factor(s)

4.2.9.1 *In silico* structure prediction and interaction with thrombin

4.2.9.1.1 Structure prediction of $NnPLA_2$-I

The best predicted structure of $NnPLA_2$-I as analyzed by I-TASSER server have been shown in Fig 4.20. The same structure was used to study the docking with human thrombin.

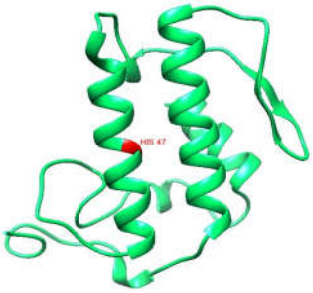

Fig 4.20. Best predicted 3D ribbon model structure of NnPLA$_2$-I by *in silico* analysis using I-TASSER server and the predicted structure was visualized by UCSF Chimera software. The active site His47 residue is highlighted in red colour.

4.2.9.1.2 Docking of NnPLA$_2$-I with human thrombin

Docking of the best predicted model of NnPLA$_2$-I with human thrombin (PDB ID: 3U69) (Fig 4.21A) demonstrated that 19 residues of NnPLA$_2$-I interacted with 25 residues of the heavy chain of thrombin via one salt bridge (red), 11 H-bonds (blue) and 148 non-bonded contacts (Fig 4.21B), with a global energy of -99.66. Out of the 19 interacting residues of NnPLA$_2$-I (Fig 4.21C), 11 residues (54 – 77) occupied the pharmacological site of elapid venom PLA$_2$ enzymes [26].

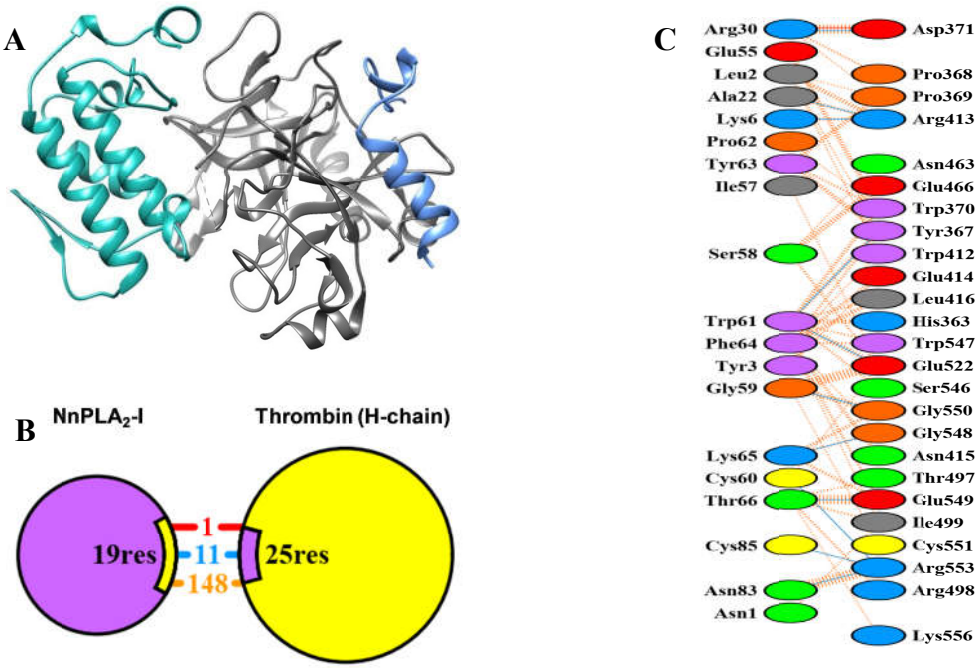

Fig 4.21. Docking of NnPLA$_2$-I with human thrombin. A. Best docking model of NnPLA$_2$-I (teal colour) and human thrombin (PDB ID: 3U69) (grey-coloured heavy

chain and blue-coloured light chain) as predicted by the ClusPro 2.0 server and refined by the Firedock server; Schematic representation of **B.** The interaction of $NnPLA_2$-I with the heavy chain of thrombin showing the different types of bonds formed between $NnPLA_2$-I and thrombin, and **C.** Residue-to-residue interactions between the two chains, as predicted by the PDBSum server. Salt bridges (ionic), H-bonds, and non-bonded contacts are represented by red, blue, and orange-coloured lines, respectively.

4.2.9.2 Spectrofluorometry assay of interaction of $NnPLA_2$-I with PC

The emission maximum of $NnPLA_2$-I observed at ~348 nm was significantly enhanced in the presence of PC (Fig 4.22A). The fluorescence intensity of $NnPLA_2$-I / PC complex was further increased when 2.0 mM Ca^{2+} was added (Fig 4.22A). It was observed that there was no difference in emission maximum between native $NnPLA_2$-I / PC complex and *p*-BPB-treated $NnPLA_2$-I / PC complex (Fig 4.22A) implying both the native as well as histidine modified PLA_2 binds with PC to an equal extent.

Interaction with PS and PE also enhanced the fluorescence intensity of $NnPLA_2$-I (Fig 4.22B).

4.2.9.3 Spectrofluorometry assay of interaction of $NnPLA_2$-I with FXa and thrombin

The interaction of $NnPLA_2$-I (50 nM) with FXa (20 nM) resulted in a significant increase in emission maximum at ~350 nm of $NnPLA_2$-I / FXa complex (Fig 4.23A); the FXa did not show any emission at the concentration used.

Further, interaction of $NnPLA_2$-I (100 nM) with thrombin (40 nM) also resulted in significant change (increase) in the fluorescence intensity of the $NnPLA_2$-I / thrombin complex (Fig 4.23B). However, the fluorescence intensity of histidine alkylated $NnPLA_2$-I / thrombin complex was found to be much less as compared to the emission maxima of $NnPLA_2$-I (unmodified) / thrombin complex (Fig 4.23B) suggesting histidine residue is essential for $NnPLA_2$-I binding to thrombin.

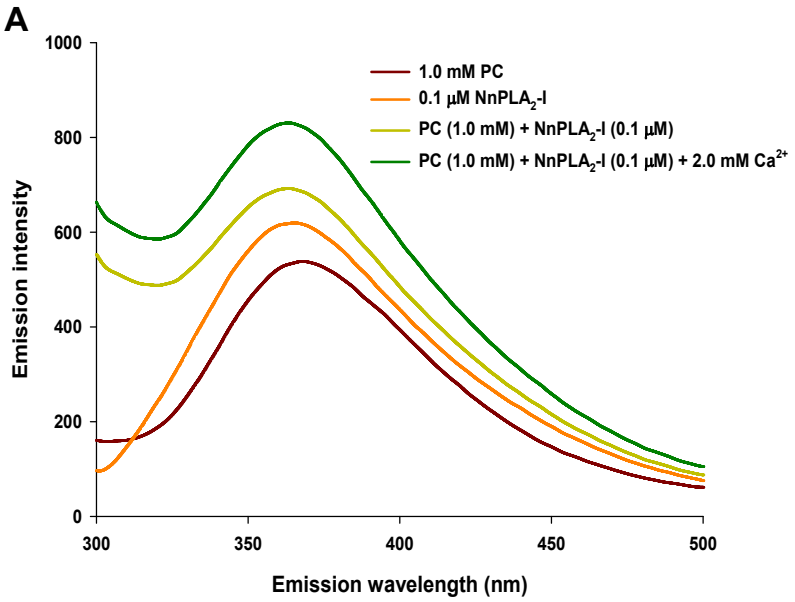

Fig 4.22A. Spectrofluorometry interaction of NnPLA$_2$-I with phospholipids. Fluorescence spectra showing interaction of native and histidine-modified NnPLA$_2$-I (0.1 µM) with phosphatidylcholine (1.0 mM) in absence and presence of Ca^{2+}. Data represent average of three determinations.

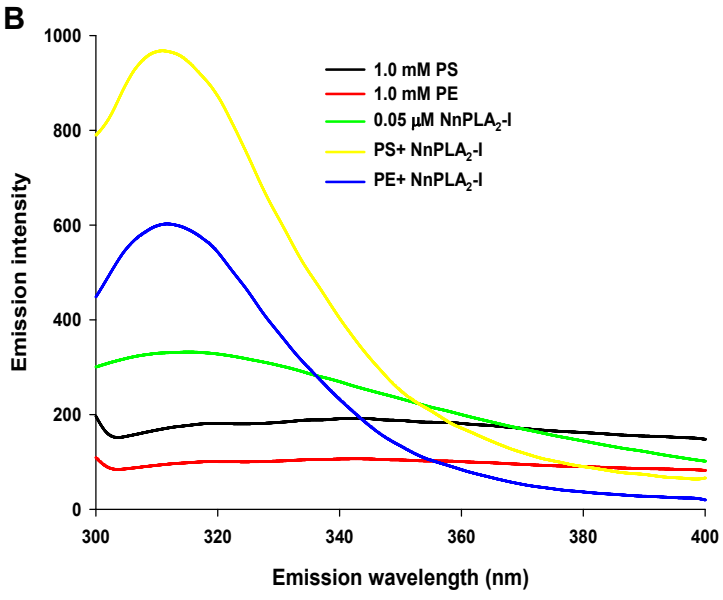

Fig 4.22B. Spectrofluorometry interaction of NnPLA$_2$-I with phospholipids (contd.). Fluorescence spectra showing interaction of native NnPLA$_2$-I (0.05 µM) with 1.0 mM of PS and PE, each. Data represent average of three determinations.

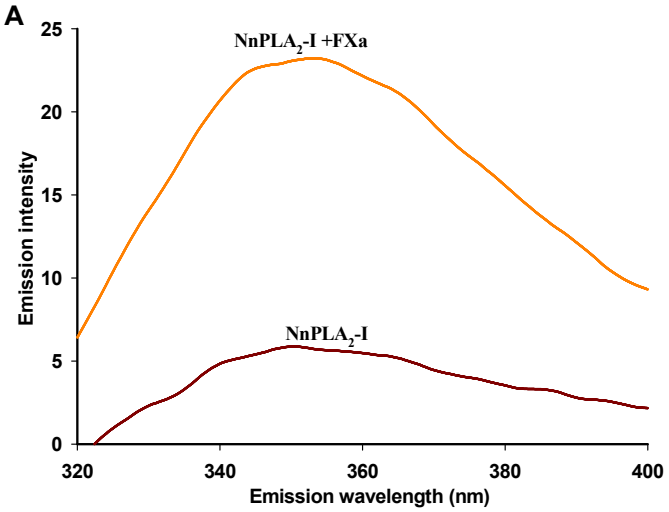

Fig 4.23A. Spectrofluorometry interaction of native NnPLA$_2$-I (50 nM) with factor Xa (20 nM). Data represent average of three determinations.

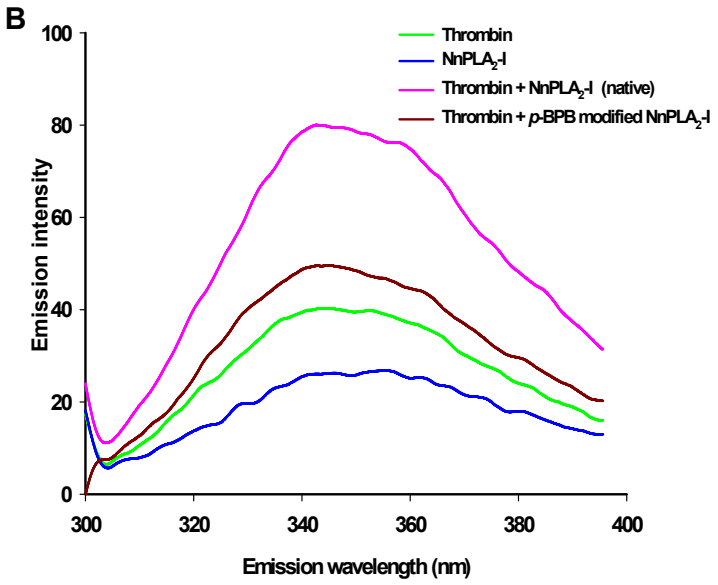

Fig 4.23B. Spectrofluorometry interaction of native and histidine-modified NnPLA$_2$-I (100 nM) with thrombin (40 nM). Data represent average of three determinations.

4.2.10 Assessment of *in vivo* toxicity and therapeutic potential of NnPLA$_2$-I

4.2.10.1 Assessment of lethality and behavioral parameters of rats

The *in vivo* toxicity assessment of NnPLA$_2$-I demonstrated that at a dose of 4.0 mg/kg it was non-lethal to rats post 72 h of intravenous (*i.v.*) injection and did not show

significant change ($p>0.05$) in the behavioral parameters of the treated group of rats as compared to control group of rats (Table 4.9).

4.2.10.2 Effect on serological parameters of blood

The serological parameters of $NnPLA_2$-I treated rats did not show any significant deviation ($p>0.05$) from control group of rats even after 72 h of injection. The different parameters that were assessed are listed in Table 4.10.

4.2.10.3 Effect on blood parameters

The different hematological parameters that were assessed in control and $NnPLA_2$-I treated rats 72 h post injection are listed in Table 4.11. As evident from the Table 4.11, no significant deviation ($p>0.05$) was observed in treated rats as compared to the control group of rats.

4.2.10.4 Effect on histological parameters

Histological analysis of major tissues (heart, kidney, and liver) of treated and untreated (control) animals did not exhibit any gross morphological difference (Fig 4.24) suggesting $NnPLA_2$-I is devoid of toxicity in rodent (Wistar rat).

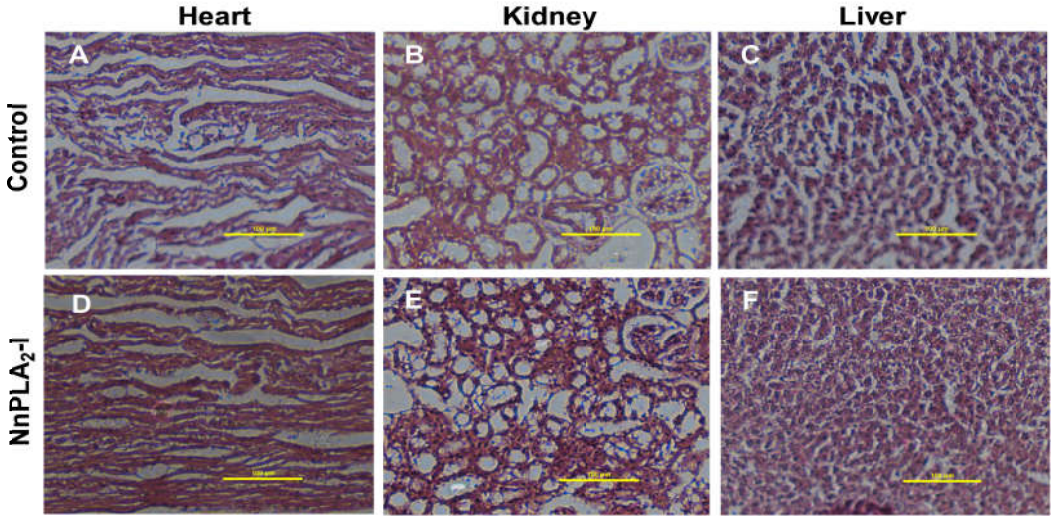

Fig 4.24. Histological images of heart, kidney, and liver tissues of Wistar strain rats treated with 4.0 mg/kg of $NnPLA_2$-I and control group of rats. After 72 h of injection, the tissues were cut from the euthanized rats, fixed, dehydrated and embedded in paraffin before sectioning, and stained with eosin-hematoxylin for histopathology study. Scale bar = 100 µm.

Table 4.9. Behavioral changes, if any, in Wistar rats after 72 h of intravenous injection of 4.0 mg/kg $NnPLA_2$-I. Values are mean ± SD of three independent determinations. Differences of values in each row are not significant ($p>0.05$).

Group of rats	Parameters									
	Body weight (g)		Grip strength (s)		Rectal temperature (F)		Fecal tendency (per 30 min)		Frequency of urination (per 30 min)	
	Initial*	Final¶	Initial*	Final¶	Initial*	Final¶	Initial*	Final¶	Initial*	Final¶
Control	140 ± 1.8	143 ± 2.1	49.5 ± 1.3	52.1 ± 0.9	95.1 ± 0.2	94.9 ± 1.6	5 ± 0.4	4 ± 0.7	4 ± 0.5	4 ± 0.8
$NnPLA_2$-I treated	141 ± 1.1	145 ± 1.4	51.6 ± 2.4	47.3 ± 1.7	94.6 ± 0.5	94.2 ± 1.1	6 ± 0.1	7 ± 0.9	7 ± 0.8	5 ± 0.3

*before injection; ¶after 72 h post injection

Table 4.10. Effect of $NnPLA_2$-I on the serum parameters of Wistar strain rats. Values are mean ± SD of three independent determinations. Differences of values in each row are not significant ($p>0.05$).

Parameter	Control	$NnPLA_2$-I
Glucose (mg/dL)	49.00 ± 2.50	68.00 ± 3.40
SGPT	115.00 ± 5.80	98.00 ± 4.90
SGOT	18.00 ± 0.90	19.00 ± 1.00
Bilirubin (mg/dL)	0.25 ± 0.02	0.29 ± 0.01
Urea (mg/dL)	3.10 ± 0.20	3.90 ± 0.20
Uric acid (mg/dL)	1.69 ± 0.10	1.07 ± 0.10
Creatinine (mg/dL)	0.10 ± 0.01	0.10 ± 0.02
Triglyceride (mg/dL)	86.60 ± 4.30	68.90 ± 3.40
Cholesterol (mg/dL)	181.30 ± 9.10	174.40 ± 8.70
LDL (mg/dL)	78.60 ± 3.90	73.10 ± 3.70
HDL (mg/dL)	20.30 ± 1.00	18.70 ± 0.90
Total protein (mg/dL)	14.41 ± 0.70	14.32 ± 0.70

Table 4.11. Effect of $NnPLA_2$-I on the blood parameters of treated Wistar rats. Values are mean ± SD of three independent determinations. Differences of values in each row are not significant ($p>0.05$).

Parameter	Control	$NnPLA_2$-I
WBC[a](m/mm^3)	5.06 ± 0.33	6.01 ± 0.13
Lymphocytes(%)	36.17 ± 1.18	34.18 ± 2.08
Monocytes(%)	5.67 ± 0.90	4.25 ± 0.80
Neutrophils(%)	50.63 ± 2.25	48.25 ± 2.15

Eosinophils(%)	10.63 ± 0.15	9.81 ± 0.19
Basophils(%)	0.10 ± 0.01	0.16 ± 0.01
Total RBC[b](m/mm^3)	8.77 ± 0.04	8.94 ± 0.30
MCV[c](fl)	44.23 ± 1.22	42.15 ± 2.10
HCt[d](%)	36.20 ± 1.80	34.35 ± 2.10
MCH[e](pg)	15.77 ± 0.18	16.28 ± 0.54
MCHC[f](g/dl)	37.13 ± 1.09	34.21 ± 1.72
RDW[g]	15.73 ± 1.06	13.25 ± 1.06
Hb[h](g/dl)	12.7 ± 0.03	12.40 ± 0.18
MPV[i](fl)	6.93 ± 0.16	7.10 ± 0.15
PCt[j](%)	0.31 ± 0.01	0.34 ± 0.01
PDW[k]	8.37 ± 0.40	7.94 ± 0.80

[a] white blood corpuscles; [b]red blood corpuscles; [c]mean corpuscular volume expressed in femtolitre; [d]hematocrit value; [e]mean corpuscular hemoglobin expressed in picograms; [f]MCH concentration expressed in gram per deciliter; [g]red blood cell distribution width; [h]hemoglobin content expressed in gram per deciliter; [i]mean platelet volume in femtolitre; [j] platelet crit; [k] platelet distribution width.

4.2.10.5 Assessment of *in vivo* anticoagulant property of NnPLA$_2$-I

Post 1 h of injection, the tail bleeding time was recorded for the control and treated rats and it was found that NnPLA$_2$-I prolonged the clotting time of blood (Table 4.12) like argatroban, but higher than that of heparin. Similar observations were obtained for TT of NnPLA$_2$-I treated rats (Table 4.12). However, re-calcification time, APTT, and PT of NnPLA$_2$-I treated rats were found to be higher as compared to the commercial anticoagulants (Table 4.12).

Table 4.12. Comparison of *in vivo* anticoagulant activity of $NnPLA_2$-I, argatroban, and heparin in Wistar strain rats. Values are mean ± SD of six independent determinations. Significance of difference *p<0.01 as compared to control and ¶p<0.05 as compared to argatroban.

Sample	PT	INR[a]	APTT	INR	TT	Ca^{2+} clotting time	Tail bleeding time
Control	17.20 ± 0.4	1.00	30.32 ± 0.1	1.00	63.01 ± 0.1	79.93 ± 1.9	61.11 ± 5.3
$NnPLA_2$-I (0.4 mg/kg)	31.84 ± 0.8*¶	1.85	44.04 ± 0.1*¶	1.45	107.45 ± 3.4*	165.86 ± 7.6*¶	152.19 ± 9.3*¶
Argatroban (0.4 mg/kg)	27.81 ± 0.8*	1.62	37.91 ± 0.4*	1.25	106.18 ± 0.6*	107.43 ± 2.8*	154.56 ± 10.2*
Heparin (0.4 mg/kg)	23.84 ± 0.6*¶	1.39	34.73 ± 1.0	1.15	93.22 ± 3.7*	97.48 ± 2.9*	120.13 ± 6.5*¶

[a] international normalized ratio (INR) = Value of treated sample / value of control

4.3 Discussion

During the past decades, significant progress has been made to explain the structure-function properties of both catalytically active and inactive snake venom PLA_2 enzymes [27-29]. It has been reported that this important class of venom molecules exerts pharmacological effects by distinctly different mechanisms, and apparently many controversial conclusions have been drawn [21]. The *N. naja* venom PLA_2 enzymes either did not show anticoagulant activity, or they were reported to possess weak anticoagulant action on PPP. In the present study, we report the purification and characterization of an acidic PLA_2 enzyme ($NnPLA_2$-I) possessing strong anticoagulant activity from venom of Indian cobra *N. naja*. Further, effort has also been given to explore the mechanism of anticoagulant action of $NnPLA_2$-I.

During the process of gel filtration, the remaining anticoagulant proteins of *N. naja* venom were separated in peaks other than in an NnCM1GF5 fraction. Therefore, the NnCM1GF5 fraction showed a lower fold of purification of anticoagulant activity compared to that of the PLA_2 activity. The molecular weight of snake venom PLA_2 enzyme is generally reported in the range of 10 to 15 kDa [10,12,13,16,21]; therefore, the molecular mass of $NnPLA_2$-I is typical of the size of PLA_2 enzymes isolated from snake venom. The identity of $NnPLA_2$-I with classical PLA_2 enzymes from cobra venom was confirmed by LC-MS/MS analysis, which may unambiguously be considered as a unique approach to identify unknown protein / peptide. The presence of putative conserved domains of the PLA_2–like superfamily reinforces the conclusion that $NnPLA_2$-I is a PLA_2 enzyme purified from *N. naja* venom. Moreover, like classical PLA_2 enzymes from snake venom, the catalytic activity of $NnPLA_2$-I was also inhibited by histidine inhibitor *p*-BPB suggesting the presence of histidine in the active site of $NnPLA_2$-I [10-13,16,17].

The PLA_2 enzymes, on the basis of their strengths to prolong the re-calcification time of PPP, are classified into groups of weak or strong anticoagulant enzymes [21,30]. The $NnPLA_2$-I can show an anticoagulant effect at a dose of 20 nM, thus suggesting that it is a strong anticoagulant enzyme [13,16,17]. This is in a close agreement to the previous reports showing that it is not the overall positive or negative charge on the venom PLA_2 molecule but rather the nature of charge in the anticoagulant site of this

group of enzyme that is the sole determinant of its anticoagulant potency [15,17,21]. The anticoagulant region is positively charged in strong anticoagulant PLA_2 enzymes, but negatively charged in weak and non-anticoagulant enzymes [31].

The anticoagulant action of snake venom PLA_2 enzymes is either fully or partially dependent on their catalytic (phospholipids hydrolysis) activity such that no uniform mechanism could be proposed [10-13,15-17,31]. Our study suggests that, similar to our previous reports on PLA_2 enzymes purified from Russell's viper and *N. kaouthia* venoms [13,15-17], the anticoagulant mechanism of $NnPLA_2$-I is partially dependent on its catalytic activity (~20% of the total anticoagulant activity shown by $NnPLA_2$-I), and to a major extent is executed through a non-catalytic mechanism via thrombin inhibition. It is well known that plasma phospholipids play a crucial role in the formation of several coagulation complexes. Very low but specific hydrolysis of plasma phospholipids through the catalytic mechanism of $NnPLA_2$-I might lead to the destruction of the specific phospholipid surface that accounts for the anticoagulant effect of this enzyme [13,15,16,21]. It is noteworthy that hydrolysis of very low but specific plasma phospholipids is the characteristic feature of strong anticoagulant PLA_2s, whereas non-specific, non-anticoagulant PLA_2 enzymes hydrolyze the plasma phospholipids at random [13,14,21].

One of the most important factors influencing the anticoagulant potency is the penetrating property of PLA_2 enzymes [15,17,21,32]. Intrinsic fluorescence distinguishes the phospholipases according to their affinity for phospholipids, and a significant increase in fluorescence signal post binding of $NnPLA_2$-I with PC vesicles, even in absence of Ca^{2+}, suggests its high penetrating ability that in turn reflects its strong anticoagulant activity [13,14,17]. This enhanced fluorescence signal may be correlated with Trp quenching in $NnPLA_2$-I, and Ca^{2+} might promote a better interaction of this PLA_2 with PC resulting in an increase in the fluorescence signal in the presence of this ion [14,17].

The non-catalytic mechanism for the anticoagulant action of snake venom PLA_2 is executed by competing with blood clotting factors such as Xa, Va, or prothrombinase complex in the lipid surface [17,21]. $NnPLA_2$-I shows a unique example of activation of amidolytic activity of FXa without influencing its prothrombin activating property. This

is further evidenced by the fact that $NnPLA_2$-I did not increase the PT of PPP therefore suggesting it does not impede the extrinsic pathways possible due to non-binding of $NnPLA_2$-I with coagulation factors such as V, VII, and X; however, it needs to be verified experimentally. Conversely, increase in APTT of PPP by $NnPLA_2$-I suggests that it inhibits intrinsic and common pathways of coagulation to exert its anticoagulant activity. The interaction of $NnPLA_2$-I with FXa probably allosterically activates the catalytic activity of the latter towards its small chromogenic substrate [33]; however, this activation might not be sufficient to enhance the catalytic activity of FXa towards its large physiological substrate prothrombin.

To date only a few thrombin inhibitor PLA_2 enzymes have been purified and characterized from snake venoms [13,16,18,34]. Since thrombin catalyzes the key step of blood coagulation cascade; therefore, thrombin is a key pharmaceutical target for the management and / or prevention of thrombotic associated disorders [35-38]. Sadly, classical anticoagulant drugs such as heparin and warfarin demonstrate several side effects including bleeding complications that suggest the search for new anticoagulants [39-42]. Notably, potent anticoagulants derived from snake venom have shown the potential to be developed as better antithrombotic prototypes [16,33,43]. The non-cytotoxic PLA_2 molecules showing thrombin inhibitory activity may therefore hold great promise for pharmaceutical application in the treatment and / or prevention of various cardiovascular disorders such as thrombosis [35]. The present study suggests that, like anticoagulant PLA_2s from *N. haje* [34], *D. russelii* [13] and *N. kaouthia* [16] venoms, $NnPLA_2$-I partially exerts its anticoagulant activity by non-covalent binding to thrombin at a site other than its heparin binding exosite-II [35]. As evident from the docking studies, the binding of $NnPLA_2$-I to thrombin is mediated by its 'pharmacological site' which resides within the 54-77 region of anticoagulant PLA_2s [26,31]. Besides, $NnPLA_2$-I also induces a conformational change in the AT-III to activate it, in a way similar to heparin, which in turn inhibits the binding of thrombin with fibrinogen. This effect leads to a greater anticoagulant effect of the $NnPLA_2$-I / AT-III complex [35]. Furthermore, similar to PLA_2 from *N. haje* venom, $NnPLA_2$-I is also found to be a mixed inhibitor of thrombin, although the strength of thrombin inhibition by $NnPLA_2$-I is superior to PLA_2 from *N. haje* venom [34], or $RVAPLA_2$

from *D. russelii* venom [13], and comparable to that of NkPLA$_2$β from *N. kaouthia* [16].

Previous studies have shown that heparin, which is a sulfated glycosaminoglycan, binds to snake venom PLA$_2$ enzymes to neutralize their various pharmacological properties such as cytotoxicity, myonecrosis, anticoagulant activity, and edema-induction [44-47]. These studies suggest the advantage of applying a low concentration of heparin as a complementary treatment against various snake envenomations [44,46]. Notably, heparin does not neutralize the phospholipids hydrolysis activity of NnPLA$_2$-I. Therefore, this indicates that heparin does not bind to the catalytic site of this enzyme or interfere with the phospholipids or membrane binding property of NnPLA$_2$-I. In 1994, Lomonte et al. [44] also reported that the interaction of myotoxin III (purified from *Bothrops asper* venom) with heparin significantly eliminated its myotoxicity without inhibiting its enzymatic activity. Therefore, partial neutralization of antithrombin activity of NnPLA$_2$-I without affecting its enzymatic activity in the presence of low molecular weight heparin supports the dissociation of catalytic and anticoagulant (pharmacological) regions in most of the snake venom PLA$_2$ molecules [11-13,17,21].

It has been shown that residues 105–118 possessing strongly cationic sites in the C-terminal loop of Lys49 myotoxin II purified from the venom of *Bothrops asper* are responsible for binding with negatively charged heparin and subsequent blocking of its myotoxicity [44]. Nevertheless, unlike the C-terminal region of myotoxic PLA$_2$s, the site containing residues 54–77 in snake venom PLA$_2$ molecule is responsible for showing anticoagulant activity [21]. In strongly anticoagulant PLA$_2$ molecules, this region is positively charged, located on the surface of the enzyme, and is accessible for interaction with the pharmacological target [21]. Although the pharmacological site of NnPLA$_2$-I is neutral in charge, it may be postulated that the positive residues in the anticoagulant region of NnPLA$_2$-I bind with the negatively charged heparin through electrostatic interaction resulting in neutralization of the thrombin inhibiting property of NnPLA$_2$-I [47].

Platelet coagulation is an important hemostatic mechanism and therefore, modulation of platelet functioning by a snake venom toxin may have an adverse effect

on envenomed prey / victims [22,48-50]. Large numbers of snake venom PLA_2 enzymes are known to influence the platelet aggregation property [4,51,52]. Based on their platelet modulating activity, venom PLA_2 enzymes can be categorized in three groups: group I PLA_2s show aggregation of platelets, group II PLA_2s inhibit the platelet aggregation induced by several physiological agents, whereas group III PLA_2s show dose-dependent platelet aggregation and deaggregation properties [52]. Therefore, $NnPLA_2$-I may be classified as a member of the group II snake venom PLA_2 enzymes.

The role of catalytic activity in platelet modulating property of $NnPLA_2$-I is evidenced by the fact that washed platelet is unaffected by this PLA_2 enzyme; nevertheless, supplementation of PPP (a source of phospholipids) or purified PC / PS to the platelets suspension resulted in formation of lysophospholipids from the hydrolysis of phospholipids by added $NnPLA_2$-I which in turn shows platelet deaggregation and inhibition of collagen-induced platelet aggregation [53]. Moreover, complete loss of platelet deaggregating property of $NnPLA_2$-I following alkylation of histidine residue indicates that the catalytic activity of $NnPLA_2$-I is involved in its platelet deaggregation [4]. Heparin, on the other hand, did not influence the antiplatelet activity of $NnPLA_2$-I owing to the fact that it does not influence the catalytic activity of this PLA_2. Moreover, the concentration of low molecular mass heparin used in this study does not show any adverse effect on platelet function may be due to formation of an antithrombin-heparin complex [54]; therefore, therapeutic application of low dose heparin besides antivenom therapy for hospital management of snakebite may be suggested. Notably, in terms of platelet binding property, $NnPLA_2$-I shows similarity to a PLA_2 purified from *N. nigricollis* venom which also demonstrates lower affinity for membrane phospholipids after histidine modification [55]. Conversely, histidine modification does not interfere with the membrane binding property of *N. kaouthia* PLA_2s [10].

Although many PLA_2s from snake venom have been shown to possess cytotoxicity [56,57], the absence of *in vitro* hemolytic activity, cell cytotoxicity, and antibacterial activity of $NnPLA_2$-I may correlate with our previous observations regarding PLA_2 enzymes purified from Indian cobra and Russell's viper venom [12-14]. It has been suggested that the biochemical properties of PLA_2 enzymes, the availability of PC in a PLA_2-sensitive membrane and / or various physicochemical properties of a

cell membrane are the major factors that show the venom PLA_2-induced membrane damage [10,12,14,58].

Strong anticoagulant potency of $NnPLA_2$-I in animal model is suggestive of development of drug prototypes for treatment of cardiovascular diseases. Drug prototypes, in the form of peptides, from the thrombin binding region of $NnPLA_2$-I may be designed and developed for assessment of their anticoagulant potency.

Bibliography:

[1] Mukherjee, A. K. and Maity, C. R. The composition of *Naja naja* venom samples from three districts of West Bengal, India. *Comparative Biochemistry and Physiology Part A- Molecular and Integrative Physiology*, 119(2): 621-627, 1998.

[2] Mukherjee, A. K. and Maity, C. R. Biochemical composition, lethality and pathophysiology of venom from two cobras- *Naja naja* and *N. kaouthia*. *Comparitive Biochemistry and Physiology Part B- Biochemistry and Molecular Biology*, 131(2): 125-132, 2002.

[3] Rudrammaji, L. M. and Gowda, T. V. Purification and characterization of three acidic, cytotoxic phospholipases A_2 from Indian cobra (*Naja naja naja*) venom. *Toxicon*, 36(6): 921-932, 1998.

[4] Satish, S., Tejaswini, J., Krishnakantha, T. P., and Gowda, T. V. Purification of a Class B1 platelet aggregation inhibitor phospholipase A_2 from Indian cobra (*Naja naja*) venom. *Biochimie*, 86(3): 203-210, 2004.

[5] Dutta, S., Chanda, A., Kalita, B., Islam, T., Patra, A., and Mukherjee, A. K. Proteomic analysis to unravel the complex venom proteome of eastern India *Naja naja*: Correlation of venom composition with its biochemical and pharmacological properties. *Journal of Proteomics*, 156: 29-39, 2017.

[6] Chanda, A., Kalita, B., Patra, A., Senevirathne, W., and Mukherjee, A. K. Proteomic analysis and antivenomics study of Western India *Naja naja* venom: Correlation

between venom composition and clinical manifestations of cobra bite in this region. *Expert Review of Proteomics*, 16(2):171-184, 2018.

[7] Chanda, A., Patra, A., Kalita, B., and Mukherjee, A. K. Proteomics analysis to compare the venom composition between *Naja naja* and *Naja kaouthia* from the same geographical location of eastern India: Correlation with pathophysiology of envenomation and immunological cross-reactivity towards commercial polyantivenom. *Expert Review of Proteomics*, 15(11): 949-961, 2018.

[8] Shashidharamurthy, R., Jagadeesha, D. K., Girish, K. S., and Kemparaju, K. Variations in biochemical and pharmacological properties of Indian cobra (*Naja naja naja*) venom due to geographical distribution. *Molecular and Cellular Biochemistry*, 229(1-2): 93-101, 2002.

[9] Shashidharamurthy, R., Mahadeswaraswamy, Y. H., Ragupathi, L., Vishwanath, B. S., and Kemparaju, K. Systemic pathological effects induced by cobra (*Naja naja*) venom from geographically distinct origins of Indian peninsula. *Experimental Toxicologic Pathology*, 62(6): 587-592, 2010.

[10] Doley, R., King, G. F., and Mukherjee, A. K. Differential hydrolysis of erythrocyte and mitochondrial membrane phospholipids by two phospholipase A_2 isoenzymes (NK-PLA_2-I and NK-PLA_2-II) from the venom of the Indian monocled cobra *Naja kaouthia*. *Archives of Biochemistry and Biophysics*, 425(1): 1-13, 2004.

[11] Doley, R. and Mukherjee, A. K. Purification and characterization of an anticoagulant phospholipase A_2 from Indian monocled cobra (*Naja kaouthia*) venom. *Toxicon*, 41(1): 81-91, 2003.

[12] Mukherjee, A. K. Correlation between the phospholipids domains of the target cell membrane and the extent of *Naja kaouthia* PLA_2-induced membrane damage: evidence of distinct catalytic and cytotoxic sites in PLA_2 molecules. *Biochimica et Biophysica Acta - General Subjects*, 1770(2): 187-195, 2007.

[13] Mukherjee, A. K. A major phospholipase A_2 from *Daboia russelii russelii* venom shows potent anticoagulant action via thrombin inhibition and binding with plasma phospholipids. *Biochimie*, 99: 153-161, 2014.

[14] Saikia, D., Bordoloi, N. K., Chattopadhyay, P., Choklingam, S., Ghosh, S. S., and Mukherjee, A. K. Differential mode of attack on membrane phospholipids by an acidic phospholipase A_2 (RVVA-PLA_2-I) from *Daboia russelli* venom. *Biochimica et Biophysica Acta-Biomembranes*, 1818(12): 3149-3157, 2012.

[15] Saikia, D., Majumdar, S., and Mukherjee, A. K. Mechanism of *in vivo* anticoagulant and haemolytic activity by a neutral phospholipase A_2 purified from *Daboia russelii russelii* venom: correlation with clinical manifestations in Russell's Viper envenomed patients. *Toxicon*, 76: 291-300, 2013.

[16] Mukherjee, A. K., Kalita, B., and Thakur, R. Two acidic, anticoagulant PLA_2 isoenzymes purified from the venom of monocled cobra *Naja kaouthia* exhibit different potency to inhibit thrombin and factor Xa via phospholipids independent, non-enzymatic mechanism. *PLoS One*, 9(8): e101334, 2014.

[17] Saikia, D., Thakur, R., and Mukherjee, A. K. An acidic phospholipase A_2 (RVVA-PLA_2-I) purified from *Daboia russelli* venom exerts its anticoagulant activity by enzymatic hydrolysis of plasma phospholipids and by non-enzymatic inhibition of factor Xa in a phospholipids/Ca^{2+} independent manner. *Toxicon*, 57(6): 841-850, 2011.

[18] Saikia, D. and Mukherjee, A. K. Anticoagulant and membrane damaging properties of snake venom phospholipase A_2 enzymes. In Gopalakrishnakone P., Inagaki H., Vogel CW., Mukherjee A., Rahmy T., editors, *Snake Venoms, Toxinology*, pages 87-104. Springer, Dordrecht, 2017.

[19] Gowda, V. T., Schmidt, J., and Middlebrook, J. L. Primary sequence determination of the most basic myonecrotic phospholipase A_2 from the venom of *Vipera russelli*. *Toxicon*, 32(6): 665-673, 1994.

[20] Kini, R. M. Excitement ahead: structure, function and mechanism of snake venom phospholipase A_2 enzymes. *Toxicon*, 42(8): 827-840, 2003.

[21] Kini, R. M. Anticoagulant proteins from snake venoms: structure, function and mechanism. *Biochemical Journal*, 397(3): 377-387, 2006.

[22] Lu, Q., Clemetson, J. M., and Clemetson, K. J. Snake venoms and hemostasis. *Journal of Thrombosis and Haemostasis*, 3(8): 1791-1799, 2005.

[23] Bhat, M. K. and Gowda, T. V. Isolation and characterization of a lethal phospholipase A_2 (NN-IVb1-PLA_2) from the Indian cobra (*Naja naja naja*) venom. *Biochemistry International*, 25(6): 1023-1034, 1991.

[24] Machiah, D. K. and Gowda, T. V. Purification of a post-synaptic neurotoxic phospholipase A_2 from *Naja naja* venom and its inhibition by a glycoprotein from *Withania somnifera*. *Biochimie*, 88(6): 701-710, 2006.

[25] Shashidharamurthy, R. and Kemparaju, K. Region-specific neutralization of Indian cobra (*Naja naja*) venom by polyclonal antibody raised against the eastern regional venom: A comparative study of the venoms from three different geographical distributions. *International Immunopharmacology*, 7(1): 61-69, 2007.

[26] Kini, R. M. and Evans, H. J. Structure-function relationships of phospholipases. The anticoagulant region of phospholipases A_2. *Journal of Biological Chemistry*, 262(30): 14402-14407, 1987.

[27] Liu, Q., Huang, Q., Teng, M., Weeks, C. M., Jelsch, C., Zhang, R., and Niu, L. The crystal structure of a novel, inactive, lysine 49 PLA_2 from *Agkistrodon acutus* venom: an ultrahigh resolution, *Ab initio* structure determination. *Journal of Biological Chemistry*, 278(42): 41400-41408, 2003.

[28] Tsai, I.-H., Wang, Y.-M., Cheng, A. C., Starkov, V., Osipov, A., Nikitin, I., Makarova, Y., Ziganshin, R., and Utkin, Y. cDNA cloning, structural, and functional analyses of venom phospholipases A_2 and a Kunitz-type protease inhibitor from steppe viper *Vipera ursinii renardi*. *Toxicon*, 57(2): 332-341, 2011.

[29] Yang, Z. M., Guo, Q., Ma, Z. R., Chen, Y., Wang, Z. Z., Wang, X. M., Wang, Y. M., and Tsai, I. H. Structures and functions of crotoxin-like heterodimers and acidic phospholipases A_2 from *Gloydius intermedius* venom: Insights into the origin of neurotoxic-type rattlesnakes. *Journal of Proteomics*, 112: 210-223, 2015.

[30] Verheij, H. M., Boffa, M. C., Rothen, C., Bryckaert, M. C., Verger, R., and de Haas, G. H. Correlation of enzymatic activity and anticoagulant properties of phospholipase A_2. *European Journal of Biochemistry*, 112(1): 25-32, 1980.

[31] Kini, R. M. Structure-function relationships and mechanism of anticoagulant phospholipase A_2 enzymes from snake venoms. *Toxicon*, 45(8): 1147-1161, 2005.

[32] Condrea, E., Fletcher, J. E., Rapuano, B. E., Yang, C. C., and Rosenberg, P. Effect of modification of one histidine residue on the enzymatic and pharmacological properties of a toxic phospholipase A_2 from *Naja nigricollis* snake venom and less toxic phospholipases A_2 from *Hemachatus haemachatus* and *Naja atra* snake venoms. *Toxicon*, 19(1): 61-71, 1981.

[33] Thakur, R., Kumar, A., Bose, B., Panda, D., Saikia, D., Chattopadhyay, P., and Mukherjee, A. K. A new peptide (Ruviprase) purified from the venom of *Daboia russelii russelii* shows potent anticoagulant activity via non-enzymatic inhibition of thrombin and factor Xa. *Biochimie*, 105: 149-158, 2014.

[34] Osipov, A. V., Filkin, S. Y., Makarova, Y. V., Tsetlin, V. I., and Utkin, Y. N. A new type of thrombin inhibitor, noncytotoxic phospholipase A_2, from the *Naja haje* cobra venom. *Toxicon*, 55(2-3): 186-194, 2010.

[35] Bode, W. Structure and interaction modes of thrombin. *Blood Cells, Molecules and Disease*, 36(2): 122-130, 2006.

[36] Mackman, N. Triggers, targets and treatments for thrombosis. *Nature*, 451(7181): 914-918, 2008.

[37] Weitz, J. I. Factor Xa or thrombin: is thrombin a better target? *Journal of Thrombosis and Haemostasis*, 5: 65-67, 2007.

[38] Steinberg, M. and Nemerson, Y. Prothrombin Activation, Thrombin, and Fibrinogen. In Colman, R.W., Marder, V.J., Clowes, A.W., George, J.N., Goldhaber, S.Z., editors, *Hemostasis and Thrombosis, Basic Principles and Clinical Practice,* pages 91-99. J.B. Lippincott Co., Philadelphia, 1982.

[39] Schulman, S., Beyth, R. J., Kearon, C., and Levine, M. N. Hemorrhagic complications of anticoagulant and thrombolytic treatment: American College of Chest Physicians Evidence-Based Clinical Practice Guidelines (8th Edition). *Chest*, 133: 257S-298S, 2008.

[40] Jacek, G. Risks and benefits of warfarin versus new oral anticoagulant drugs. *Home Healthcare Now*, 35(4): 231-232, 2017.

[41] Warkentin, T. E., Roberts, R. S., Hirsh, J., and Kelton, J. G. Heparin-induced skin lesions and other unusual sequelae of the heparin-induced thrombocytopenia syndrome: a nested cohort study. *Chest*, 127(5): 1857-1861, 2005.

[42] Harr, T., Scherer, K., Tsakiris, D. A., and Bircher, A. J. Immediate type hypersensitivity to low molecular weight heparins and tolerance of unfractioned heparin and fondaparinux. *Allergy*, 61(6): 787-788, 2006.

[43] Mukherjee, A. K. Green medicine as a harmonizing tool to antivenom therapy for the clinical management of snakebite: the road ahead. *Indian Journal of Medical Research*, 136(1): 10-12, 2012.

[44] Lomonte, B., Tarkowski, A., Bagge, U., and Hanson, L. A. Neutralization of the cytolytic and myotoxic activities of phospholipases A_2 from *Bothrops asper* snake venom by glycosaminoglycans of the heparin/heparan sulfate family. *Biochemical Pharmacology*, 47(9): 1509-1518, 1994.

[45] Landucci, E. C., Toyama, M., Marangoni, S., Oliveira, B., Cirino, G., Antunes, E., and de Nucci, G. Effect of crotapotin and heparin on the rat paw oedema

induced by different secretory phospholipases A_2. *Toxicon*, 38(2): 199-208, 2000.

[46] Rostelato-Ferreira, S., Leite, G. B., Cintra, A. C. O., da Cruz-Höfling, M. A., Rodrigues-Simioni, L., and Oshima-Franco, Y. Heparin at low concentration acts as antivenom against *Bothrops jararacussu* venom and bothropstoxin-I neurotoxic and myotoxic actions. *Journal of Venom Research*, 1: 54, 2010.

[47] Perchuc, A. M., Menin, L., Favreau, P., Bühler, B., Bulet, P., Schöni, R., Wilmer, M., Ernst, B., and Stöcklin, R. Isolation and characterization of two new Lys49 PLA_2s with heparin neutralizing properties from *Bothrops moojeni* snake venom. *Toxicon*, 55(6): 1080-1092, 2010.

[48] Koh, D., Armugam, A., and Jeyaseelan, K. Snake venom components and their applications in biomedicine. *Cellular and Molecular Life Sciences*, 63(24): 3030-3041, 2006.

[49] Marsh, N. and Williams, V. Practical applications of snake venom toxins in haemostasis. *Toxicon*, 45(8): 1171-1181, 2005.

[50] Matsui, T., Fujimura, Y., and Titani, K. Snake venom proteases affecting hemostasis and thrombosis. *Biochimica et Biophysica Acta - Protein Structure and Molecular Enzymology*, 1477(1-2): 146-156, 2000.

[51] Silveira, L. B., Marchi-Salvador, D. P., Santos-Filho, N. A., Silva, F. P., Jr., Marcussi, S., Fuly, A. L., Nomizo, A., da Silva, S. L., Stabeli, R. G., Arantes, E. C., and Soares, A. M. Isolation and expression of a hypotensive and anti-platelet acidic phospholipase A_2 from *Bothrops moojeni* snake venom. *Journal of Pharmaceutical and Biomedical Analysis*, 73: 35-43, 2013.

[52] Cherifi, F., Namane, A., and Laraba-Djebari, F. Isolation, functional characterization and proteomic identification of CC2-PLA_2 from *Cerastes cerastes* venom: a basic platelet-aggregation-inhibiting factor. *Protein Journal*, 33(1): 61-74, 2014.

[53] Yuan, Y., Jackson, S. P., Newnham, H. H., Mitchell, C. A., and Salem, H. H. An essential role for lysophosphatidylcholine in the inhibition of platelet aggregation by secretory phospholipase A_2. *Blood*, 86(11): 4166-4174, 1995.

[54] Salzman, E. W., Rosenberg, R. D., Smith, M. H., Lindon, J. N., and Favreau, L. Effect of heparin and heparin fractions on platelet aggregation. *Journal of Clinical Investigation*, 65(1): 64-73, 1980.

[55] Prigent-Dachary, J., Boffa, M., Boisseau, M., and Dufourcq, J. Snake venom phospholipases A_2. A fluorescence study of their binding to phospholipid vesicles correlation with their anticoagulant activities. *Journal of Biological Chemistry*, 255(16): 7734-7739, 1980.

[56] Chanda, C., Sarkar, A., Sistla, S., and Chakrabarty, D. Anti-platelet activity of a three-finger toxin (3FTx) from Indian monocled cobra (*Naja kaouthia*) venom. *Biochemical and Biophysical Research Communications*, 441(3): 550-554, 2013.

[57] Khunsap, S., Pakmanee, N., Khow, O., Chanhome, L., Sitprija, V., Suntravat, M., Lucena, S. E., Perez, J. C., and Sánchez, E. E. Purification of a phospholipase A_2 from *Daboia russelii siamensis* venom with anticancer effects. *Journal of Venom Research*, 2: 42, 2011.

[58] Mukherjee, A., Ghosal, S., and Maity, C. Lysosomal membrane stabilization by α-tocopherol against the damaging action of *Vipera russelli* venom phospholipase A_2. *Cellular and Molecular Life Sciences*, 53(2): 152-155, 1997.